



HAL
open science

Cocrystals of Nitrofurantoin: How Coformers Can Modify Its Solubility and Permeability Across Intestinal Cell Monolayers

Alekos Segalina, Barbara Pavan, Valeria Ferretti, Federico Spizzo, Giada Botti, Anna Bianchi, Mariachiara Pastore, Alessandro Dalpiaz

► **To cite this version:**

Alekos Segalina, Barbara Pavan, Valeria Ferretti, Federico Spizzo, Giada Botti, et al.. Cocrystals of Nitrofurantoin: How Coformers Can Modify Its Solubility and Permeability Across Intestinal Cell Monolayers. *Crystal Growth & Design*, 2022, 22 (5), pp.3090-3106. 10.1021/acs.cgd.2c00007. hal-03871099

HAL Id: hal-03871099

<https://hal.science/hal-03871099>

Submitted on 25 Nov 2022

HAL is a multi-disciplinary open access archive for the deposit and dissemination of scientific research documents, whether they are published or not. The documents may come from teaching and research institutions in France or abroad, or from public or private research centers.

L'archive ouverte pluridisciplinaire **HAL**, est destinée au dépôt et à la diffusion de documents scientifiques de niveau recherche, publiés ou non, émanant des établissements d'enseignement et de recherche français ou étrangers, des laboratoires publics ou privés.



Distributed under a Creative Commons Attribution 4.0 International License

Co-Crystals of nitrofurantoin: how the co-formers can modify its solubility and permeability across intestinal cell monolayers

Alekos Segalina, Barbara Pavan,* Valeria Ferretti, Federico Spizzo, Giada Botti, Anna Bianchi, Mariachiara Pastore* and Alessandro Dalpiaz

AUTHOR INFORMATION

Corresponding Authors

Barbara Pavan - Department of Neuroscience and Rehabilitation - Section of Physiology, University of Ferrara, via L. Borsari 46, I-44121 Ferrara, Italy; orcid: 0000-0001-8942-9310; *E-mail*: pvnbb@unife.it

Mariachiara Pastore - Laboratoire de Physique et Chimie Théoriques, Université de Lorraine & CNRS, Boulevard des Aiguillettes, BP 70239 54506 Vandoeuvre-lès-Nancy Cedex, France; *E-mail*: mariachiara.pastore@gmail.com

Authors

Alekos Segalina - Laboratoire de Physique et Chimie Théoriques, Université de Lorraine & CNRS, Boulevard des Aiguillettes, BP 70239 54506 Vandoeuvre-lès-Nancy Cedex, France.

Valeria Ferretti - Department of Chemical, Pharmaceutical and Agricultural Sciences, University of Ferrara, via Fossato di Mortara 19, I-44121 Ferrara, Italy.

Federico Spizzo - Department of Physics and Earth Sciences, University of Ferrara, Via Saragat, 1 – I-44122 Ferrara, Italy.

Giada Botti - Department of Chemical, Pharmaceutical and Agricultural Sciences, University of Ferrara, via Fossato di Mortara 19, I-44121 Ferrara, Italy.

Anna Bianchi - Department of Chemical, Pharmaceutical and Agricultural Sciences, University of Ferrara, via Fossato di Mortara 19, I-44121 Ferrara, Italy.

Alessandro Dalpiaz - Department of Chemical, Pharmaceutical and Agricultural Sciences, University of Ferrara, via Fossato di Mortara 19, I-44121 Ferrara, Italy.

ABSTRACT: Solubility and permeability of nitrofurantoin (NITRO) were compared with those of its co-crystals containing isoniazid (ISO), bipyridyl (BIP) or phenanthroline (PHE) as co-formers, and their parent mixtures. NITRO dissolution profiles were evaluated via HPLC; we resorted to molecular dynamics (MD) simulations to rationalize the experimental data on the basis of nitrofurantoin-co-formers and nitrofurantoin-water intermolecular interactions. Permeation studies were performed by using an *in vitro* model of small intestine based on IEC-6 cells. The NITRO water solubility was reduced by its mixture with PHE and BIP, but not with ISO. Co-crystallization with BIP induced a slight increase of NITRO solubility; co-crystallization with PHE induced its solubility decrease, even if lower than the physical mixture. The solubility changes were attributed to NITRO solvation shell alterations (MD simulations). Co-crystallization with ISO allowed to increase the NITRO solubility in the first 30 minutes of dissolution pattern. Permeation measurements showed that the NITRO-PHE mixture was detrimental for the monolayer integrity, whereas no alterations were induced by the co-crystal. No effects on NITRO permeability and monolayer integrity were observed neither for NITRO-ISO nor for NITRO-BIP mixtures. NITRO-ISO co-crystal increased the NITRO permeability across the monolayer without reducing its integrity.

KEYWORDS: *co-crystals; physical mixtures; nitrofurantoin; drug permeation; molecular dynamics*

1. INTRODUCTION

A great percentage of market drugs are poorly water soluble, with a main distribution in Class II (low solubility–high permeability) and Class IV (low solubility–low permeability),¹⁻⁴ according to the Biopharmaceutics Classification System (BCS).⁵ In particular, drugs showing poor water solubility are included in about 40% of approved pharmaceutical products for oral administration and nearly in 90% of discovery pipeline formulations.⁶ These types of drugs are therefore often characterized by poor oral bioavailability.¹ The low water solubility of drugs requires, therefore, new strategies in order to obtain bioavailability improvements of oral formulations.¹ Taking into account that the lattice energy of a solid form influences its solubility (lower solubility is induced by higher energy), the use of amorphous forms may seem an appropriate strategy in order to increase the bioavailability of poorly water-soluble drugs.³ On the other hand, the poor stability and the tendency to recrystallize over time limit the use of amorphous forms in pharmaceutical industry.⁷ Alternatively, salts represent more than 50% of administered drugs, but their use is not possible for non-ionizable drugs.⁸ Among the new crystal engineering strategies, co-crystallization appears promising to solve the bioavailability problems of poorly water-soluble drugs, being potentially able to improve their solubility and retaining, at the same time, the typical stability of crystalline compounds in the solid state.³

Co-crystals are very similarly defined by EMA (*“homogenous crystalline structures made up of two or more components in a defined stoichiometric ratio where the arrangement in the crystal lattice is not based on ionic bonds”*⁹) and FDA (*“crystalline materials which are composed of two or more molecules in the same crystalline lattice and associated by non-ionic and non-covalent bonds”*¹⁰), even if the regulatory status regarding their use in pharmaceutical products is still unsettled.^{3,4,9,10}

These crystalline constructions are known to increase the solubility and bioavailability of poorly water-soluble drugs, even if this is not systematic.¹¹⁻¹³ Moreover, recent works indicate that

co-crystals can modify the permeability properties of drugs.¹ As a matter of fact, most of these studies were performed by using artificial membranes, such as dialysis, silicon, or polyvinylidene fluoride (PVDF), where the ability of co-crystals to modify the permeability of an active pharmaceutical ingredient (API) was attributed to the drug-co-former interactions,¹⁴⁻¹⁸ or to the changed solubility of drugs.¹⁹⁻²¹ Other studies evidenced the co-crystal incapacity to alter the drug permeability across the artificial membranes.²² Few studies across skin evidenced the ability of co-crystals to enhance the API permeability, and this property was attributed to the co-former lipophilicity or to the increased solubility of drugs.^{23,24} Finally, permeation studies with co-crystals were proposed by using cell monolayers, obtained by Caco-2 or Calu-3 cellular lines; in particular, some co-crystals appeared able to increase the permeability of APIs across the monolayers and this phenomenon was attributed to the inhibitory power of co-formers toward active efflux systems of the cells,^{25,26} or to the modification of the structure and intermolecular bonding of APIs by the co-crystallization.²⁷ Other studies did not evidence effects on permeability by co-formers or co-crystals on cell monolayers.²² About the permeation across cell monolayers, we have evidenced that indomethacin and carbamazepine co-crystals can induce marked differences in influencing the integrity of intestinal cell monolayers, if compared with the pure drugs and the parent physical mixtures.^{28,29} This phenomenon was studied by using several types of co-formers, independently of their clinical relevance, evidencing that in physiologic environments the properties of co-crystals and their parent physical mixtures can be strongly different from each other. As an example, the mixture of indomethacin with saccharin appeared detrimental for the integrity of intestinal cell monolayers, whereas the parent co-crystal was able to preserve its integrity; vice versa, the co-crystal of indomethacin with 2-hydroxy-4-methylpyridine was detrimental for the integrity of intestinal cell monolayers, whereas the parent mixture did not influence its integrity;²⁸ again, carbamazepine and its mixtures with vanillic acid, succinic acid or 4-nitropyridine N-oxide significantly perturbed the integrity of intestinal cell monolayers that was instead preserved by the parent co-crystals.²⁹ Our results suggest, therefore, that co-crystals dissolved in water can appear as

entities totally different than their parent physical mixtures, being able to produce different effects about the stability and permeability of intestinal monolayers. Taking into account these aspects, we have proposed that it is not always true that pharmaceutical co-crystals (where at least one of the co-formers is an API and the other is pharmaceutically acceptable¹²), being able to modify the physicochemical properties of drugs without altering their molecular structures, can retain their therapeutic and safety properties, as currently believed.^{3,4,30}

In this paper we perform further investigations on the different properties between co-crystals and parent physical mixtures, taking into account their potential different effects on physiologic environments. In particular, we prepared new co-crystals or salts of nitrofurantoin, a widely used antibacterial drug that FDA approved for the treatment of the lower urinary tract infection.³¹ After oral administration, nitrofurantoin is partially excreted unchanged in the urine, where it exhibits a bacteriostatic activity at the minimum inhibitory concentration (MIC = 32 $\mu\text{g/mL}$ ³²), or a bactericide action at concentrations higher than 2 x MIC.³³ Nitrofurantoin is also characterized by low solubility in water (about 100 $\mu\text{g/mL}$ at 25°C³⁴), and it is defined as a Class IV compound.^{34,35} Therefore, the dissolution in gastro-intestinal fluids and permeation across intestinal barrier appear to be the critical time-dependent steps of its absorption following oral administration.³⁶

Several polymorphic forms are related to nitrofurantoin: anhydrous (α or β) and hydrate (I or II).³⁷ The anhydrous stable commercial form (β polymorph) is known to be transformed, in the presence of water, into the more stable monohydrate II form, which shows the lowest dissolution rate³⁸ and influences the solubility of the anhydrous nitrofurantoin.³⁸ It is indeed known that the dissolution rate and bioavailability of anhydrous nitrofurantoin decreases during time in the presence of humidity,³⁹ but also that co-crystals of nitrofurantoin with 4-aminobenzoic acid, urea, and L-arginine can improve its physicochemical properties.^{34,35}

For our study, we prepared co-crystals of nitrofurantoin with isoniazid and other co-formers without clinical relevance (2-aminopyrimidine, 2-hydroxy-4-methylpyridine, 4-aminopyrimidine, betahistine – salt, 2,6-diaminopyridine - salt) in order to investigate, from a general point of view, if co-crystals and parent physical mixtures can induce different effects in physiologic environments. The co-crystals and salts obtained with co-formers without clinical relevance were characterized by scarce reproducibility, so their experimental investigation was limited to the crystallographic analysis.

The new co-crystal obtained with isoniazid was used together with two previously described co-crystals with bipyridyl (BIP) and phenanthroline (PHE)⁴⁰ to investigate their ability to influence the solubility of nitrofurantoin and its permeability of intestinal cell monolayers in comparison with the parent physical mixtures. Despite BIP and PHE co-formers are not appropriate to obtain pharmaceutical co-crystals, we used them to investigate, from a general point of view, if the components of co-crystals solubilized in water can induce biological effects (e.g. on NITRO permeability across cell monolayers or on their tight junction stability) different than those obtained by the solubilized parent physical mixtures. The schematic representation of nitrofurantoin and the co-formers used for this study is reported in Figure 1.

Following the computational protocol that we developed in Ref. (29), the experimental data are integrated with theoretical investigations, based on classical molecular dynamics (MD) simulations of the drug and its co-formers in their stoichiometric ratio in the case of co-crystals (COC) and at different concentrations, according to their relative solubility, for the physical mixtures (MIX). These calculations served as a basis to get atomistic insights on the observed change in the drug solubility, allowing to track the nature and the strength of the intramolecular interactions in water environment between the nitrofurantoin and the different co-formers.

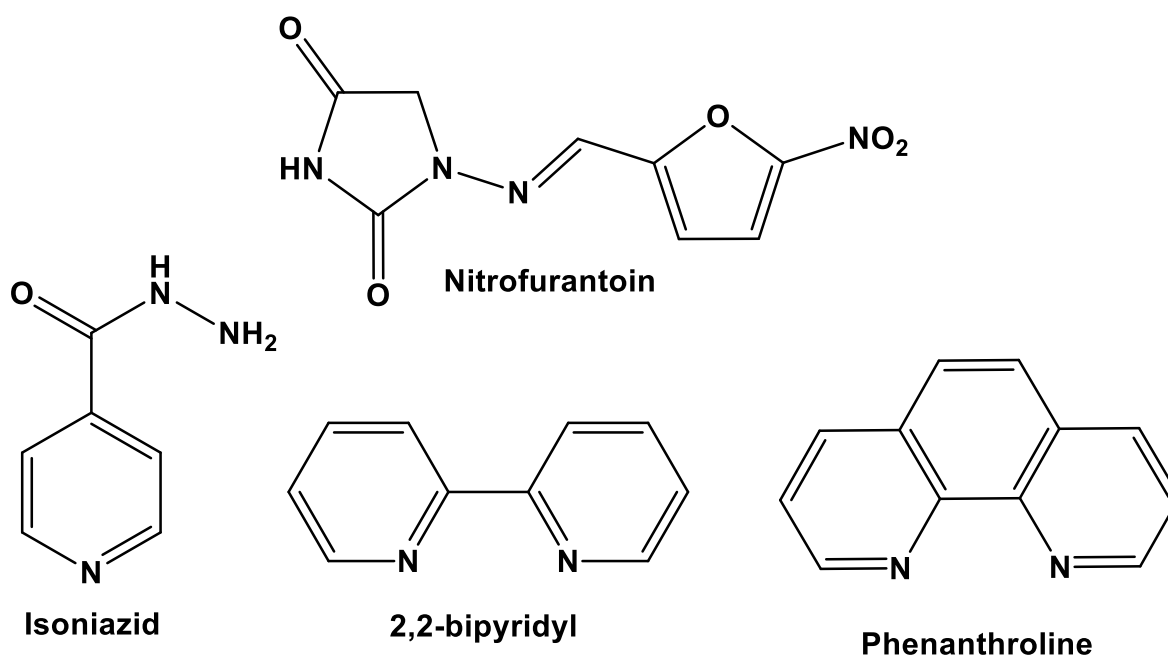


Figure 1. Schematic representation of nitrofurantoin and the co-formers isoniazid, 2,2'-bipyridyl and 1,10-phenanthroline in co-crystals NITRO-ISO, NITRO-BIP and NITRO-PHE, respectively.

2. MATERIALS AND METHODS

2.1. Materials. Nitrofurantoin, 2,2'-bipyridyl, 1,10-phenanthroline, isoniazid, N,N'-dimethylformamide (anhydrous) and ethanol (absolute alcohol) were obtained from Sigma Aldrich (Milan, Italy). Acetonitrile and water were of high-performance liquid chromatography (HPLC) grade from Sigma-Aldrich. Dulbecco's modified Eagle's medium (DMEM) + Glutamax, fetal bovine serum (FBS), penicillin, streptomycin, trypsin, phosphate buffered saline (PBS) and trypsin-EDTA were obtained from ThermoFisher Scientific- Life Technologies (Monza, Italy). The IEC-6 cell line was obtained from Sigma Aldrich, following terms and conditions of supply of products from the Culture Collections of Public Health England (Culture Collections) comprising of the European Collection of Authenticated Cell Cultures (ECACC). The 12-well Millicell inserts were obtained from Millipore (Milan, Italy). All other reagents and solvents were of analytical grade (Sigma Aldrich).

2.2. Synthesis of Adducts. Six new co-crystals or salts containing nitrofurantoin have been synthesized and characterized by X-ray crystallography: (1) nitrofurantoin/isoniazid monohydrate 2:1:1 (NITRO-ISO); (2) nitrofurantoin/2-aminopyrimidine 1:1; (3) nitrofurantoin/2-hydroxy-4-methylpyridine 1:1; (4) nitrofurantoin/4-aminopyrimidine monohydrate 1:1:1; (5) nitrofurantoin/betahistine 1:1 (salt); (6) nitrofurantoin/2,6-diaminopyridine 1:1 (salt). Beside salts, co-crystals containing 2-aminopyrimidine, 2-hydroxy-4-methylpyridine and 4-aminopyrimidine were used in the present work only for crystallographic analysis. Indeed, we made several attempts to obtain appreciable amounts of these products with a good purity level, using both the solvent slow-evaporation and grinding techniques, but the X-ray powder diffraction spectra of the obtained powders pointed out they were not pure enough.

The nitrofurantoin/isoniazid (NITRO-ISO) and nitrofurantoin/2,2'-bipyridyl (NITRO-BIP) co-crystals have been obtained by slow evaporation of a solution of drug/isoniazid or drug/bipyridyl in 2:1 molar ratio, using as solvent N,N'-dimethylformamide and a mixture of ethanol/N,N'-dimethylformamide 50:50 (v/v), respectively. The nitrofurantoin/phenanthroline (NITRO-PHE) co-crystal has been obtained by dissolution of an equimolar quantity of co-formers in the minimum quantity of acetonitrile. The solutions were left for slow evaporation at room temperature after mild heating and crystals were observed after a few days. The other co-crystals and salts were prepared by dissolving equimolar quantities of nitrofurantoin and the co-formers in a mixture of ethanol/N,N'-dimethylformamide 50:50 (v/v), in a sufficient amount to ensure full dissolution. The crystallizing dishes containing the solutions were partially covered to allow the slow evaporation of the solvent at room temperature. The crystals appeared after few days.

The phase and composition of the three co-crystals NITRO-ISO, NITRO-PHE and NITRO-BIP have been checked by X-ray powder crystallography, comparing the experimental spectra with those calculated from the single-crystal crystallography structures.

2.3. X-Ray Diffraction. The crystallographic data for the six co-crystals/salts were collected on a Nonius Kappa CCD diffractometer at room temperature using graphite-monochromated MoK α radiation ($\lambda = 0.71073 \text{ \AA}$). Data sets were integrated with the Denzo-SMN package⁴¹ and corrected for Lorentz-polarization effects. The structures were solved by direct methods with the SIR97 suite of programs⁴² and refinement was performed on F^2 by full-matrix least-squares methods with all non-hydrogen atoms anisotropic. All calculations were performed using SHELXL-2018⁴³ implemented in the WINGX system of programs.⁴⁴

Powder diffraction spectra for the pure compounds nitrofurantoin, isoniazid, phenanthroline, bipyridyl and for both co-crystals and physical mixtures NITRO-ISO, NITRO-PHE and NITRO-BIP before and after incubation in PBS (see section 2.8) were recorded, at room temperature, on a Bruker D-8 Advance diffractometer with graphite monochromatized Cu K α radiation ($\lambda = 1.5406 \text{ \AA}$). The data were recorded at 2θ steps of 0.02° with 1 s/step.

The ORTEPIII⁴⁵ diagram of nitrofurantoin/isoniazid is shown in Figure 2; experimental details and hydrogen bonding parameters are given in Tables 1 and 2, respectively. A detailed description of single-crystal data collection and refinement for all other new co-crystals are reported in the Supporting Information. In particular, ORTEPIII⁴⁵ diagrams, experimental data for single-crystal diffraction and hydrogen bonding parameters are given in Figures S1-S5, Table S1 and Table S2, respectively. Supporting Information report also the powder diffraction spectra for co-crystals NITRO-ISO, NITRO-PHE and NITRO-BIP (Figures S6-S8).

Crystallographic data for the structural analysis of the six new compounds have been deposited at the Cambridge Crystallographic Data Center, 12 Union Road, Cambridge, CB2 1EZ, UK, and are available free of charge from the Director on request quoting the deposition number CCDC 2002482-2002487 for compounds 1-6, respectively.

Table 1. Experimental Details of NITRO-ISO Co-Crystal.

Chemical formula	2(C ₈ H ₆ N ₄ O ₅).C ₆ H ₇ N ₃ O.H ₂ O
M_r	631.50
Crystal system, space group	Monoclinic, Cc
Temperature (K)	295
a, b, c (Å)	19.9687 (6), 6.5355 (2), 20.3184 (6)
α, β, γ (°)	90, 92.010 (2), 90
V (Å ³)	2650.0 (1)
Z	4
Radiation type	Mo $K\alpha$
μ (mm ⁻¹)	0.13
No. of measured, independent and observed [$I > 2\sigma(I)$] reflections	14615, 6707, 5322
R_{int}	0.043
$R[F^2 > 2\sigma(F^2)], wR(F^2), S$	0.041, 0.104, 1.04
No. of reflections/No. parameters	6707/490
$\Delta\rho_{max}, \Delta\rho_{min}$ (e Å ⁻³)	0.20, -0.19

Table 2. Hydrogen Bonding Parameters; D= donor, A= acceptor (Å, °) of NITRO-ISO Co-Crystal.

	D -H	D ...A	H ...A	<D -HA
N3-H ...O5A	1.00(3)	3.041(3)	2.22(3)	136(3)
O1W-H...N1	0.93(3)	2.781(3)	1.86(3)	173(3)
N3B-H ...O1W	0.99(4)	2.824(3)	1.82(4)	177(3)
O1W-H...O5B ⁱ	0.80(4)	2.785(3)	2.00(4)	166(4)
N2-H ...O5A ⁱ	0.84(3)	3.104(3)	2.35(3)	148(3)
N3-H ...O1W ⁱⁱ	0.93(3)	3.043(3)	2.16(3)	156(2)
C4-H ...O5B	0.95(3)	3.321(3)	2.43(3)	155(3)
C5A-H...O4A ⁱ	0.91(3)	3.162(3)	2.26(3)	169(3)
C8B-H...O1 ⁱⁱⁱ	0.91(2)	3.420(3)	2.55(2)	158(2)
C5B-H...O4B ^{iv}	0.91(3)	3.298(3)	2.39(3)	170(3)

Equivalent positions: (i) $x, y-1, z$; (ii) $x, -y, z+1/2$; (iii) $x, 1-y, z-1/2$; (iv) $x, y+1, z$

2.4. Thermal Analysis. Thermal analyses on the samples were carried out on a Netzsch Thermal Analyzer (STA 409) that allows to perform simultaneous thermogravimetric and differential thermal analysis, TGA and DTA, respectively. Both the TGA and the DTA signals were calibrated using different standards (indium, tin, and zinc), in order to cover the whole range of investigated temperatures. The samples (2–4 mg) were put in non-hermetic aluminum pans and scanned at a heating rate of 10 °C/min in the 50–400 °C range under a continuous purged dry nitrogen flux (20 ml/min). The data were collected in triplicate for each sample.

2.5 Infrared Spectroscopy. Infrared spectroscopy IR spectra were obtained with a Spectrum 100 FT-IR Spectrometer controlled by Spectrum 6.1.0 on Windows platform both from Perkin Elmer (Waltham, Massachusetts, US). The spectrometer was equipped with U ATR – 1 Reflection Diamond Top-plate – ZnSe for the data acquisition and the spectral range was 7800-350 cm^{-1} . The spectra represent 8 co-added scans collected at a spectral resolution of 4 cm^{-1} . The spectrometer is a CDRH Class I, BS EN 60825-1/IEC 60825-1 Class 1 laser products. The optical module contained a Class II/2 Helium Neon (HeNe) laser, emitting visible, continuous wave radiation at a wavelength of 633 nm and had a maximum output power of 1 mW.

2.6. HPLC Analysis. Nitrofurantoin was quantified through HPLC, using a chromatographic apparatus made of a modular system (LC-10 AD VD model pump and SPD-10A VP model variable wavelength UV-Vis detector; Shimadzu, Kyoto, Japan) and completed with an injection valve provided of a 20 μL sample loop (model 7725; Rheodyne, IDEX, Torrance, CA, USA). The separation was conducted at room temperature on a Hypersil C-18 BDS reverse-phase column (150 x 4.6 mm, 5 μm) with a precolumn filled with the same separation phase (Alltech, Milan, Italy). Data were acquired and processed through CLASS-VP Software, version 7.2.1 (Shimadzu Italia, Milan, Italy) installed on a personal computer. The mobile phase was made of an acetonitrile-water mixture in an 20:80 (v:v) ratio and the flow rate was set at 1 mL/min. The UV

detector was set up at 366 nm. The retention time of nitrofurantoin at these conditions was 4.5 minutes. The chromatographic precision for nitrofurantoin was evaluated by repeated analysis (n=6) of the same sample (10 μ M – 2.4 μ g/mL) of nitrofurantoin dissolved in water; the relative standard deviation (RSD) value was 0.79%. The calibration curves of peak areas *versus* concentration of nitrofurantoin were obtained in a range from 0.5 μ M (0.12 μ g/mL) to 100 μ M (24 μ g/mL) in water and resulted linear (n = 9, r = 0.998; P < 0.0001). A preliminary analysis performed with 100 μ M solutions showed that isoniazid, phenanthroline and bipyridyl did not interfere with the retention time of nitrofurantoin.

2.7. Dissolution Studies. All the samples were micronized and then sieved through stainless standard-mesh sieves, with a mesh size of 106 μ m. In each experiment, the solid powders were poured into 12 mL of 10 mM PBS (pH 7.4) at 37 °C and incubated in a water bath under gentle shaking (100 rpm). The quantity of sieved powders used were 150.0 mg of nitrofurantoin; 198.85 mg of co-crystal NITRO-ISO; 263.43 mg of co-crystal NITRO-PHE; 199.18 mg of co-crystal NITRO-BIP; 150.0 mg of nitrofurantoin mixed with 43.18 mg of isoniazid, 124.85 mg of phenanthroline monohydrate, or 49.18 mg of bipyridyl for the parent physical mixtures NITRO-ISO, NITRO-PHE, or NITRO-BIP, respectively. Aliquots (200 μ L) were withdrawn from the suspensions at predefined time intervals, filtered through regenerated cellulose filters (0.45 μ m) and diluted 1:20 in water. 10 μ L of the treated sample were injected into the HPLC system to quantify the nitrofurantoin concentrations. The obtained values were the mean of three independent experiments.

2.8. Stability of Solubilized NITRO Co-Crystals and Physical Mixtures. The solution stability of NITRO, its co-crystals and physical mixtures in PBS 10 mM was evaluated at 37 °C at the same conditions adopted for dissolution studies. After 6 hours of incubation, the samples were

filtered, rapidly washed with purified water (4 °C), and dried, then powder X-ray diffraction spectra were recorded.

2.9. Cell Culture and Differentiation of IEC-6 cells to Polarized Monolayers. The rat normal small intestine epithelial IEC-6 cell line was grown in DMEM + Glutamax supplemented with 10% fetal bovine serum (FBS), 100 U/mL penicillin/streptomycin at 37 °C in a humidified atmosphere of 95%, with 5% of CO₂. After two passages, confluent cells were seeded in 12-well Millicell inserts consisting of 1.0 µm pore size polyethylene terephthalate (PET) filter membranes, whose surface was 1.13 cm². In particular, filters were pre-soaked for 24 h with fresh culture medium, and then the upper compartment (apical, A) received 400 µL of the diluted cells (2·10⁵ cells/mL), whereas the lower (basolateral, B) received 2 mL of the medium in the absence of cells. The exhausted growth medium was replaced with fresh medium both in the apical and basolateral compartments every second day until the cell monolayer was fully confluent and one day before starting the experiment medium was replaced on both sides of the monolayer by the medium containing low serum (1% FBS). The integrity of the cell monolayers was monitored after 24 hours by measuring the transepithelial electrical resistance (TEER, Ω·cm²) by means of a voltmeter (Millicell-ERS; Millipore, Milan, Italy). The TEER values of cell monolayers, obtained by deducing the background resistance of blank inserts not plated with cells, reached at confluence a stable value of 50 Ω·cm². The homogeneity and integrity of the cell monolayer were also monitored by phase contrast microscopy before permeation studies.

2.10. Permeation Studies Across Cell Monolayers. Inserts were washed three times with pre-warmed PBS buffer in the apical (A, 400 µL) and basolateral (B, 2 mL) compartments; PBS buffer containing 5 mM glucose at 37 °C was then added to both compartments. In this phase the TEER values of the monolayers were measured. The sieved powders were then added to the apical compartments in the following amounts: 5 mg of nitrofurantoin; 6.63 mg of co-crystal NITRO-ISO;

8.78 mg of co-crystal NITRO-PHE; 6.64 mg of co-crystal NITRO-BIP; 5 mg of nitrofurantoin mixed with 1.44 mg of isoniazid, 4.16 mg of phenanthroline monohydrate, or 1.64 mg of bipyridyl for the parent physical mixtures NITRO-ISO, NITRO-PHE, or NITRO-BIP, respectively. During permeation experiments, Millicell inserts loaded with the powders were continuously swirled on an orbital shaker (100 rpm; model 711/CT, ASAL, Cernusco, Milan, Italy) at 37 °C. At programmed time points the inserts were removed and transferred into the subsequent well containing fresh PBS; then basolateral PBS was harvested, filtered through regenerated cellulose filters (0.45 µm) and, after 1:10 dilution in water, injected (10 µL) into the HPLC system for nitrofurantoin detection and quantification. At the end of incubation the apical slurries were withdrawn, filtered, and injected into the HPLC system (10 µL) after 1:20 dilution. After the withdrawal of apical samples, 400 µL of PBS was added in the apical compartments that were inserted in the original basolateral compartments of Millicell plates filled with 2 mL of PBS, in order to perform TEER measurements. Permeation experiments were also conducted using cell-free inserts in the same conditions. The values obtained were the mean of three independent experiments. Apparent permeability coefficients (P_{app}) of nitrofurantoin were calculated according to eq 1:⁴⁶⁻⁴⁸

$$P_{app} = \frac{\frac{dc}{dt} V_r}{S_A C} \quad (1)$$

where P_{app} is the apparent permeability coefficient in cm/min; dc/dt is the flux of drug across the filters, calculated as the linearly regressed slope through linear data; V_r is the volume in the receiving compartment (basolateral = 2 mL); S_A is the diffusion area (1.13 cm²); and C is the compound concentration in the donor chamber (apical) detected at 60 min and chosen as approximate apical concentration.

2.11. Statistical Analysis about Permeation Studies. Statistical comparisons between apparent permeability coefficients of nitrofurantoin were performed by one way ANOVA followed by Dunnett's post-test; statistical comparisons between transepithelial electrical resistance before and after incubation with the sieved samples were performed by one way ANOVA followed by Bonferroni post-test. $P < 0.001$ was considered statistically significant. All the calculations were performed by using the computer program Graph Pad Prism (GraphPad Software Incorporated, San Diego, CA, USA), which was used also for the linear regression of the cumulative amounts of the compounds in the basolateral compartments of the Millicell systems. The quality of fit was determined by evaluating the correlation coefficients (r) and P values.

2.12. Computational Details. Classical MD simulations, using the generalized Amber force field (GAFF), have been performed for the nitrofurantoin alone and for binary systems composed of the drug and the three co-formers (COF), PHE, ISO and BIP, in different concentrations to simulate the co-crystallized forms (COC) and the corresponding mixtures (MIX). The point charges were obtained by fitting the electrostatic potential employing the RESP protocol at the HF/6-31G* level of theory. The systems were embedded in a periodic cubic cell ($\sim 100 \times 100 \times 100 \text{ \AA}^3$) filled by water molecules, described by the TIP3P model, in order to approximate the bulk conditions (density equal to $\sim 0.86 \text{ g/cm}^3$). Following the computational protocol employed in our previous work²⁹, to mimic the COC system we started the MD runs from small clusters cut from the COC X-ray structures keeping the experimental drug-co-former ratio: 4:4 for NITRO-PHE and 4:2 for NITRO-BIP and NITRO-ISO. A reference MD run with 4 molecules (cluster) cut from the NITRO crystal structure in the same water box was also performed. The parent physical mixtures have been simulated considering 4:20 (NITRO-BIP), 4:12 (NITRO-PHE) and 4:120 (NITRO-ISO) drug:co-former ratios that have been chosen to reflect the relative saturation concentrations of the co-formers in the mixture solutions. The simulation boxes were built by randomly distributing drug and co-former molecules using PACKMOL package⁴⁹ and ensuring that the densities of the

simulation boxes are similar among them. So, we adopted periodic boxes with a volume of $126.83 \times 120.60 \times 105.32 \text{ \AA}^3$, $110.11 \times 116.18 \times 109.57 \text{ \AA}^3$ and $130.15 \times 129.28 \times 130.071 \text{ \AA}^3$ for the NITRO-BIP, the NITRO-PHE and the NITRO-ISO mixture, respectively. For all the simulations an initial energy minimization has been carried out for 10000 cycles to remove the bad contacts, followed by thermalization conducted for 20 ps in NVT ensemble to bring the temperature to 300K and equilibration in the NPT ensemble conducted for 400 ps imposing the pressure to 1 atm. Then, the MD production runs were executed for ~ 200 ns, by setting the time step to 0.2 fs and using the RATTLE algorithm to fix the bonds involving hydrogen atoms.

All the simulations have been performed with the GPU extension of the AMBER code^{50,51} and the analysis were carried out with CPPTRAJ and VMD.

3. RESULTS

3.1. Nitrofurantoin Co-Crystals. Six new co-crystals or salts containing nitrofurantoin have been synthesized and characterized by X-ray crystallography: (1) nitrofurantoin/isoniazid monohydrate 2:1:1 (NITRO-ISO); (2) nitrofurantoin/2-aminopyrimidine 1:1; (3) nitrofurantoin/2-hydroxy-4-methylpyridine 1:1; (4) nitrofurantoin/betahistine 1:1 (salt); (5) nitrofurantoin/4-aminopyridine monohydrate 1:1:1 (salt); (6) nitrofurantoin/2,6-diaminopyridine 1:1 (salt).

According to the so-called “rule of three”, when synthesizing a mixed crystal a salt is expected if the $\Delta pK_a = (pK_a(\text{base}) - pK_a(\text{acid}))$ is greater than 2/3 units, while the formation of a cocrystals is observed if the ΔpK_a is smaller than 0.^{52,53} A ΔpK_a ranging between 0 and 3 is generally considered to be in a salt–cocrystal continuum, so that it is not possible to predict “a priori” the formation of a salt or a cocrystal.

Nitrofurantoin has an imide acidic group and its pKa value is 6.67;⁵⁴ considering the pKa of the co-formers, listed in Table S3 together with the corresponding Δ pKa values, the “rule of three” turns out to be fulfilled for all mixed crystals with the exception of the salt formed by nitrofurantoin and 2,6-diaminopyridine. In this case, however, the Δ pKa is very close to zero (-0.17). Moreover, the hydrogen of the protonated pyridine was found in the difference Fourier map and refined without any problem while, on the contrary, any attempt to find and refine a possible hydrogen bound to the nitrofurantoin nitrogen failed. It is noteworthy to mention that in all crystals the hydrogens bound to N/O atoms were located in the difference Fourier map and isotropically refined, so that to verify the proton transfer in salts.

Out of three new co-crystals, in spite of many attempts, it was possible to synthesize in appreciable quantity only the one having isoniazid as co-former, besides two adducts reported in the literature: nitrofurantoin/phenanthroline 1:1 (NITRO-PHE) and nitrofurantoin/2,2'-bipyridyl 2:1 (NITRO-BIP).⁴⁰ The crystal structure details of nitrofurantoin/2-aminopyrimidine, nitrofurantoin/2-hydroxy-4-methylpyridine, and of the three salts are reported in the Supplementary Information.

The X-ray three-dimensional structures of the three co-crystals used in the present study are shown in Figure 2; the main hydrogen-bonding interactions between the molecules are drawn as dashed lines. About the co-crystal NITRO-ISO (a), both the organic molecules constituting the crystal are almost planar. The configuration of nitrofurantoin with respect to the C=N double bond is *E*, with the C—H group pointing towards the methylene group of the imidazolidinedione ring; this same configuration is found in the pure drug crystal.

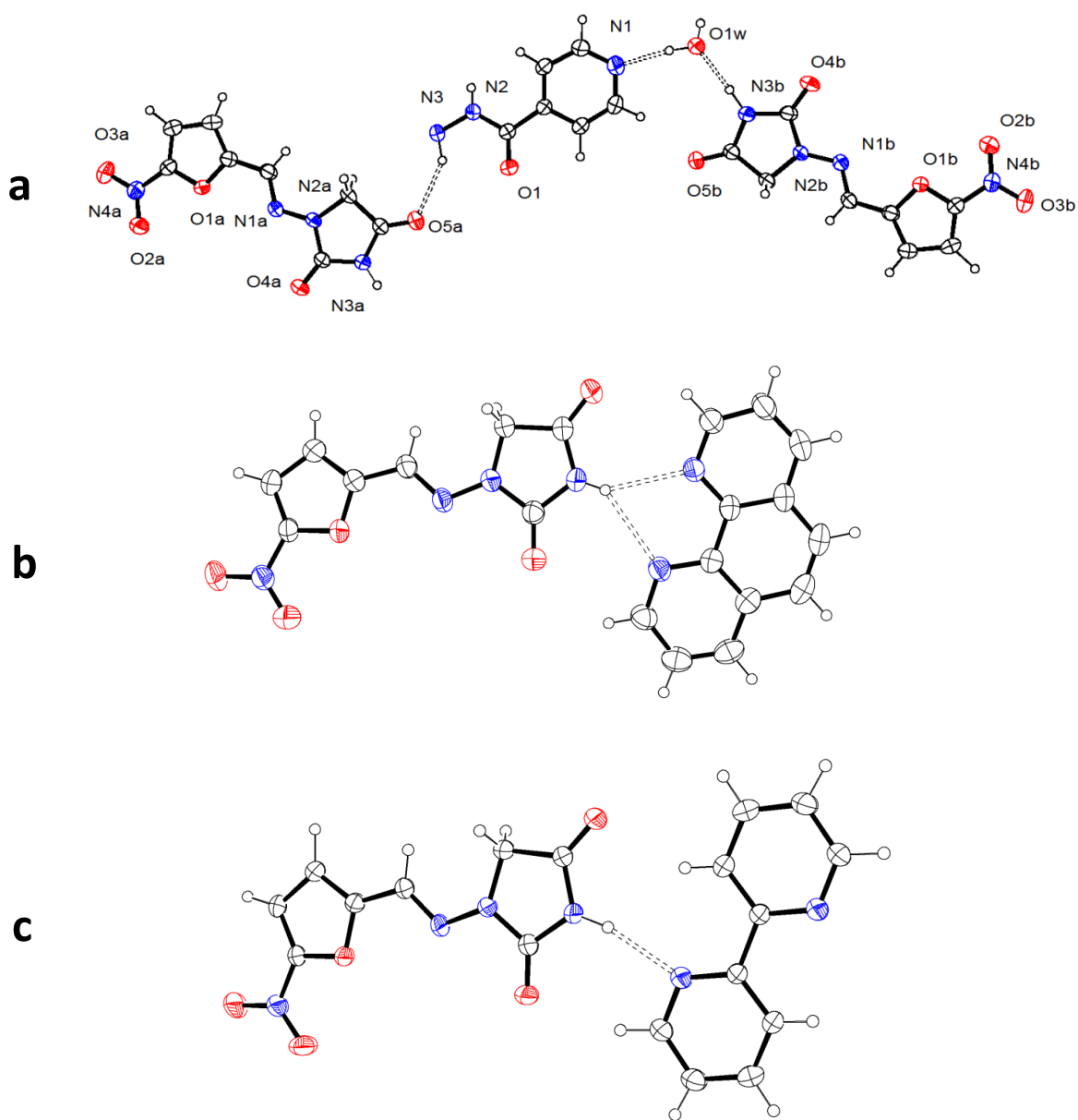


Figure 2. ORTEP⁴⁵ view for (a) nitrofurantoin/isoniazid (NITRO-ISO); (b) nitrofurantoin/phenanthroline (NITRO-PHE⁴⁰) and (c) nitrofurantoin/2,2'-bipyridyl (NITRO-BIP⁴⁰) co-crystals. Thermal ellipsoids are drawn at the 40% probability level. Hydrogen bonds are drawn as dashed lines.

In the asymmetric unit, formed by one isoniazid, two nitrofurantoin and one co-crystallized water molecules, one nitrofurantoin is directly linked to isoniazid through an N-H...O hydrogen bond, involving one of the C=O groups of the drug and the hydrazine group of the co-former, which can be classified of medium strength, according to the analysis of the distribution of N...O distances in hydrogen bonded structures.⁵⁵ Conversely, the drug/co-former interaction of the second nitrofurantoin molecule is mediated by the water that bridges the two moieties acting both as a hydrogen bonding donor and acceptor (Figure 2a and Table 2 of the Experimental section). Indeed, the water molecule plays an important role in connecting the different units in the crystal, since it is involved in four hydrogen bonds; one of them, O1W-H...N1, is remarkably strong (donor...acceptor distance = 2.781(3) Å). Although the packing architecture is mainly determined by these interactions, some weaker C-H...O hydrogen bonds also contribute to the crystal stability (Table 2). No significant $\pi\cdots\pi$ interaction has been found.

3.2 Thermal Analysis. Figure 3 reports the traces obtained by thermogravimetric (TGA) and differential thermal analysis (DTA) for nitrofurantoin and its co-crystals. The melting point of nitrofurantoin co-crystals and their co-formers, obtained by DTA, are reported in Table 3.

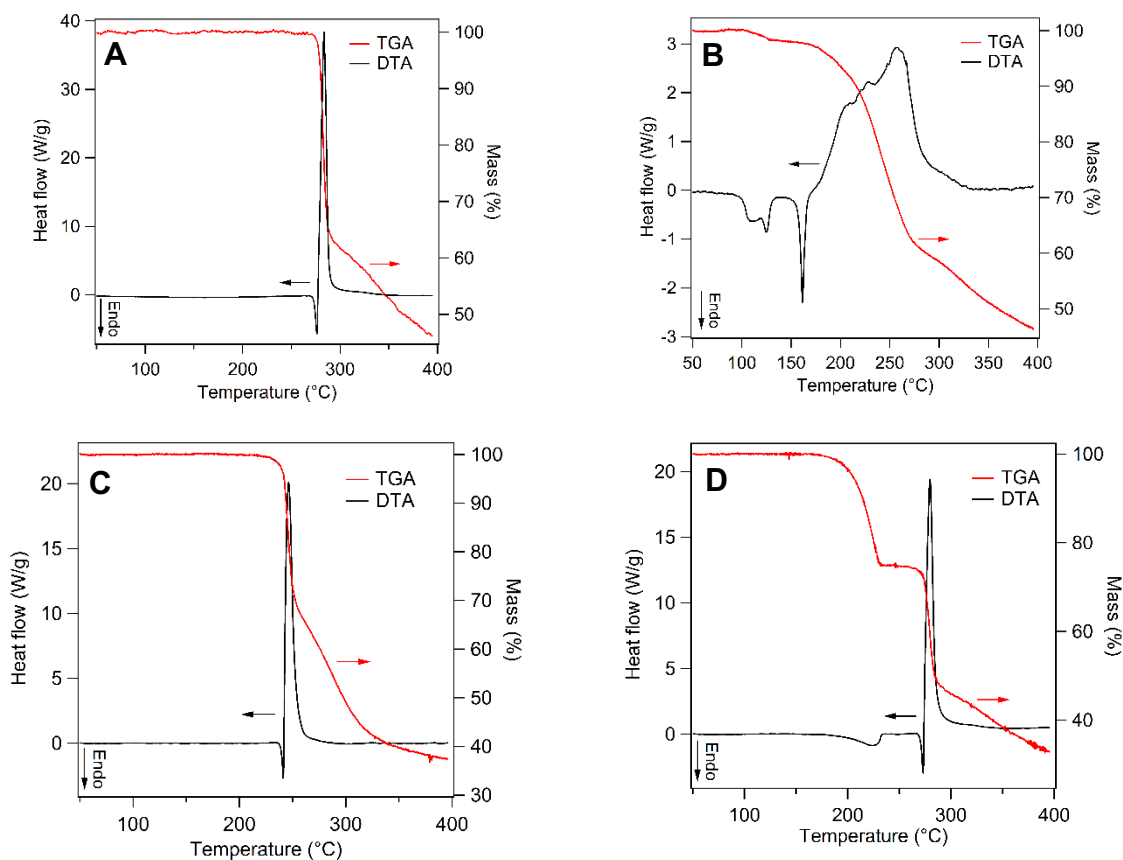


Figure 3. TGA and DTA traces obtained for pure [A] nitrofurantoin and its co-crystals [B] NITRO-ISO, [C] NITRO-PHE and [D] NITRO-BIP

Table 3. Melting Points (Onset, °C) for the NITRO Co-Crystals and Co-Formers as Determined by DTA. The Melting Point of the NITRO β -Form is $272.9 \pm 0.2^\circ \text{C}$

System	NITRO-ISO	NITRO-PHE	NITRO-BIP
Co-crystal	161.0 ± 0.2	196.5 ± 0.2	269.9 ± 0.2
Co-former	171.3 ± 0.2	118.5 ± 0.2	70.5 ± 0.2

The DTA traces evidence that nitrofurantoin undergoes melt degradation and that this property appears reproduced by its co-crystals, as previously reported for other co-crystals of this drug.^{34,56,57} As a consequence, it was not possible to accurately obtain the enthalpy of fusion of

nitrofurantoin and its co-crystals. The melting point of nitrofurantoin (272.9 °C) was higher than that of the co-crystals and their co-formers. The NITRO-PHE and NITRO-BIP co-crystals showed melting points between that of nitrofurantoin and that of the parent conformer, while the co-crystal NITRO-ISO showed a melting point lower than those of both components (Table 3). The DTA of this co-crystal evidenced endotherms at 101.6 ± 0.2 °C and 158.0 ± 0.2 °C, preliminary to melting and decomposition (161.0 ± 0.2 °C) that appear due the desolvation of the crystallization water, as observed from the weight loss of material in TGA trace (about the 3%). Moreover, the presence of isoniazid in the co-crystal seems to interfere with the decomposition of nitrofurantoin that is characterized by an enlarged DTA exothermic peak in comparison to those of pure nitrofurantoin and the other co-crystals. The DTA of the NITRO-BIP co-crystal showed an endotherm at 196.5 ± 0.2 °C prior to melting and decomposition (269.9 ± 0.2 °C) that may be attributed to the very low BIP melting point (about 70 °C) in comparison to the melting points of NITRO and its co-crystal NITRO- BIP (about 270 °C).

3.3. Infrared Spectroscopy. Figure 4 reports the FT-IR spectra obtained for the NITRO-ISO physical mixture [A] and the parent co-crystal [B]. The spectrum of the physical mixture appears as a sum of the peaks obtained by the spectra of the two pure compounds, allowing to evidence the characteristic peaks related to the β -polymorph of nitrofurantoin, whose IR spectrum is reported in Supplementary Information (Figure S9). The peaks related to the β -polymorph of nitrofurantoin in Figure 4A are evidenced at the wavenumbers 3281 cm^{-1} and 3151 cm^{-1} , indicating the N-H stretching and the vinyl C-H stretching, and at the wavenumbers 1804 cm^{-1} , 1778 cm^{-1} , 1746 cm^{-1} and 1728 cm^{-1} , representative of the carbonyl C=O stretching. Moreover, the peak at 1110 cm^{-1} appears related to the C-N stretching in the hydantoin region.⁵⁸ The spectrum of the NITRO-ISO co-crystal (Figure 4B) evidences several shifts and changes about the peaks related to pure β -polymorph of nitrofurantoin described in Figure 4A. In particular, the peaks at 1110 cm^{-1} and 3280 cm^{-1} are upshifted to 1121 and 3351 cm^{-1} , respectively and the set of peaks between 1804

and 1728 cm^{-1} appear sensibly changed. Finally, the peak related to the N3-H stretching of isoniazid (3103 cm^{-1} , Figure 4A) disappears in the co-crystal spectrum (Figure 4B).

The FT-IR spectra obtained in the presence of isoniazid are representative for those obtained in the presence of phenanthroline and bipyridyl, reported in the Supplementary Information (Figures S10 and S11).

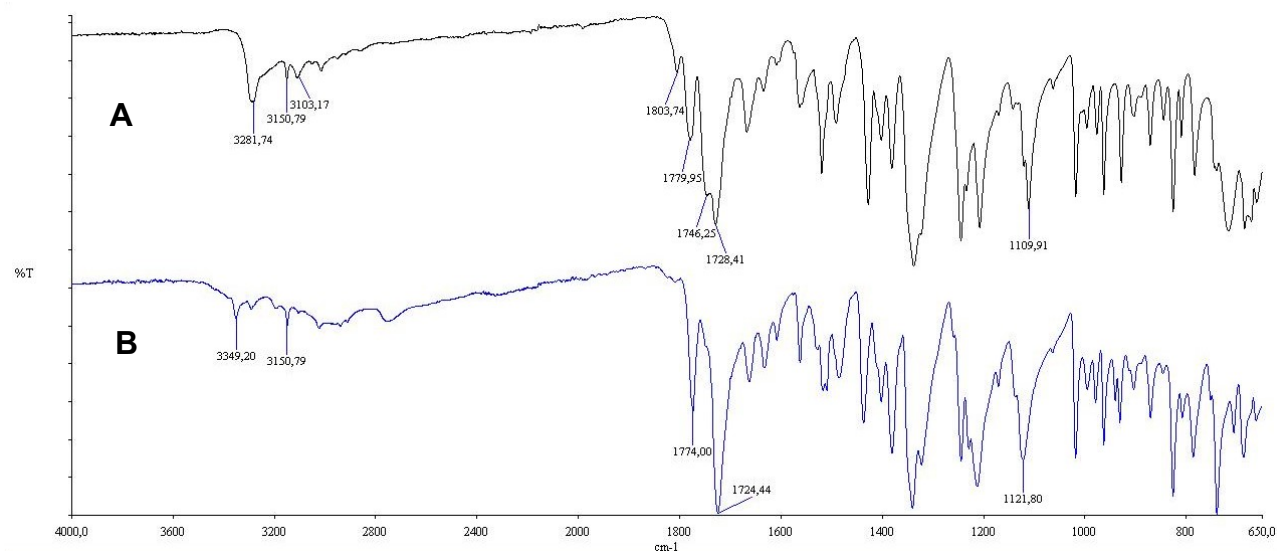


Figure 4. FT-IR spectra of NITRO-ISO physical mixture [A] and NITRO-ISO co-crystal [B].

3.4. Dissolution Studies. The dissolution profiles in 10 mM PBS at $37\text{ }^{\circ}\text{C}$ of nitrofurantoin as free drug, co-crystallized, or mixed in the parent mixtures are reported in Figure 5. The saturation concentration of free nitrofurantoin was reached within 10 min of its incubation in the buffer, showing a value of about $300\text{ }\mu\text{g/mL}$. The dissolution profile of nitrofurantoin did not appear significantly altered when mixed with isoniazid, with only a slight increase in the drug concentration (up to $370\text{ }\mu\text{g/mL}$) within 30 min of the mixture incubation; then the dissolution profile appeared overlaid to that of the free NITRO alone. On the other hand, a drastic decrease of nitrofurantoin concentration was registered when mixed with bipyridyl or phenanthroline. In particular, the drug concentrations were detected between 50 and $100\text{ }\mu\text{g/mL}$ or between 70 and $30\text{ }\mu\text{g/mL}$ during the incubation of the mixtures with bipyridyl or phenanthroline, respectively.

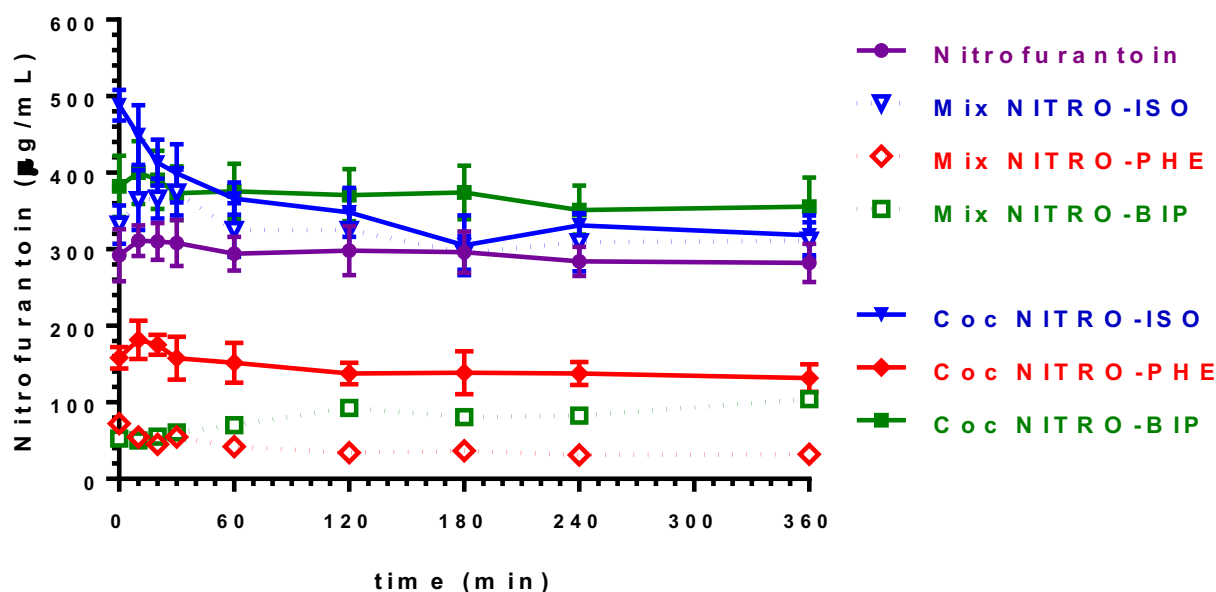


Figure 5. Solubility and dissolution profiles in PBS 10 mM at 37 °C for nitrofurantoin as free drug, or co-crystallized, or mixed in the parent mixtures. Data are reported as the mean \pm SD of three independent experiments.

The co-crystal NITRO-ISO was associated with a relative high increase of nitrofurantoin concentration during its first incubation phase. In particular, the first nitrofurantoin concentration detected during time was about 500 $\mu\text{g/mL}$, then this value slightly decreased within 2 hours up to overlaid to the dissolution profiles of the free drug or the parent physical mixture.

The co-crystal NITRO-PHE appeared able to partially counteract the drastic decrease of nitrofurantoin dissolution registered when mixed with phenanthroline, allowing to detect nitrofurantoin concentrations of about 150 $\mu\text{g/mL}$ during its incubation. Also, the NITRO-BIP co-crystal appeared able to counteract the decrease of nitrofurantoin dissolution observed for the parent mixture. In this case, the co-crystal dissolution allowed to increase the nitrofurantoin concentration up to about 400 $\mu\text{g/mL}$, evidencing, among the samples analyzed, the highest range of nitrofurantoin concentrations between the dissolution profiles of co-crystals and parent physical mixtures.

3.5. Stability of Solubilized NITRO Co-Crystals and Physical Mixtures. The stability of NITRO, its co-crystals and physical mixtures in PBS 10 mM was investigated by slurring the powders in the solvent at 37 °C for six hours, reproducing the same conditions adopted for the dissolution studies. The dried powders obtained after incubation were analyzed by X-ray diffraction, whose spectra are reported in Figures S12-S16, as a comparison with those obtained before the incubation of the powders of compound in PBS. Firstly, after incubation in PBS NITRO appeared as orthorhombic nitrofurantoin monohydrate (Figure S12).⁵⁹ The powder diffraction spectrum for NITRO-ISO mixture, obtained after its incubation in PBS, evidenced the presence of orthorhombic nitrofurantoin monohydrate (Figure S13), similarly as detected for its parent co-crystal (Figure S16A). The powder diffraction spectrum for NITRO-PHE mixture, obtained after its incubation in PBS, evidenced the presence of both orthorhombic nitrofurantoin monohydrate and pure PHE (Figure S14). On the other hand, the powder diffraction spectrum for NITRO-BIP mixture evidenced the presence of its parent co-crystal and the absence of both orthorhombic nitrofurantoin monohydrate and pure BIP (Figure S15).

The co-crystals NITRO-PHE and NITRO-BIP appeared stable at the incubation conditions adopted, being their spectra superimposable with those obtained before incubation (Figures S16B and S16C). On the other hand, the monohydrate co-crystal NITRO-ISO lost its stability during incubation, as evidenced by its spectrum not superimposable with that obtained before incubation (Figure S16A). The spectrum obtained after incubation evidenced essentially the presence of orthorhombic nitrofurantoin monohydrate.

3.6. Permeation Studies. The permeation studies of nitrofurantoin across the *in vitro* model of small intestinal wall, constituted by IEC-6 cells, were performed by using glucose enriched PBS as incubation medium. In order to simulate an oral administration, the sieved powders of nitrofurantoin, its co-crystals, or the parent mixtures were added in the apical compartment of the “Millicell” systems with the same ratio between solid powders and the same incubation medium

used for dissolution studies. For permeation studies the analysis time was 60 min for all samples. The cumulative amounts of nitrofurantoin in the basolateral receiving compartments were linear within 60 min ($n=6$, $r \geq 0.990$, $P < 0.001$), as reported in Figure 6, indicating constant permeation conditions within this range of time. The resulting slopes of the linear fits allowed to calculate the apparent permeability coefficients (P_{app}) of nitrofurantoin (Figure 7) according to equation (1), where the drug concentrations detected in the apical compartments after 1 h of incubation of the powders were used as approximate apical concentrations. These latter values were essentially in line with those obtained from dissolution studies of nitrofurantoin powders (Figure 5), so their dissolution appeared slightly influenced by the presence of the cells.

A comparison of the P_{app} values of nitrofurantoin (Figure 7) obtained in the presence ($2.24 \cdot 10^{-3} \pm 0.16 \cdot 10^{-3}$ cm/min) or in the absence ($10.90 \cdot 10^{-3} \pm 0.42 \cdot 10^{-3}$ cm/min) of IEC-6 monolayers indicated a significant lower permeation of the drug in the presence of cells than in their absence ($P < 0.001$). This difference of P_{app} values was relatively high ($8.7 \cdot 10^{-3}$ cm/min), confirming the ability of the cell monolayers to behave as a physiologic barrier. Accordingly, the TEER values measured at confluence for the IEC-6 monolayers were about $50 \Omega \cdot \text{cm}^2$ (Figure 8), as expected for this type of cell lines,⁶⁰ both in the absence (NITRO 0h) and in the presence of nitrofurantoin (NITRO 1h).

The P_{app} value of nitrofurantoin across IEC-6 monolayers did not appear altered when mixed with isoniazid and bipyridyl, as reported in Figure 7. In particular, the P_{app} values of nitrofurantoin

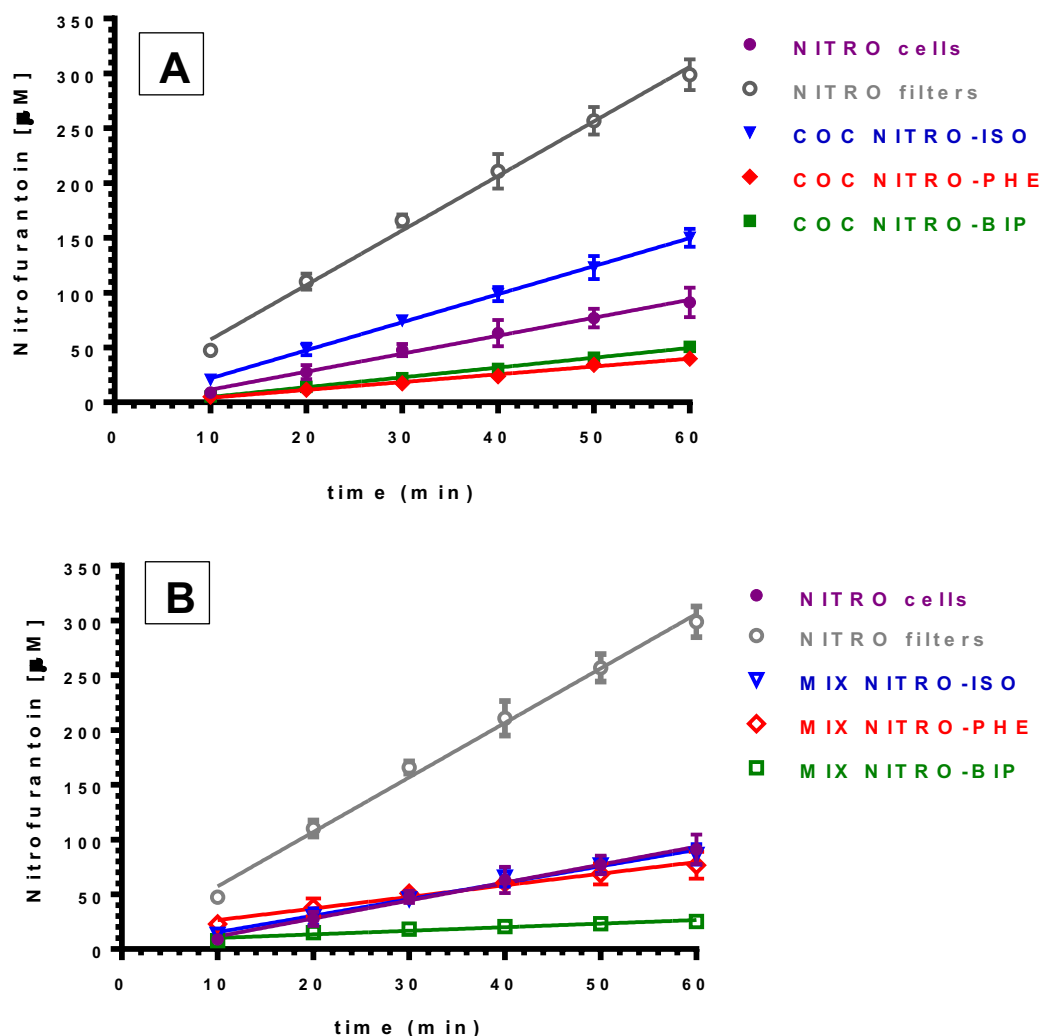


Figure 6. Permeation kinetics of nitrofurantoin after introduction in the “Millicell” apical compartments of powders constituted by free nitrofurantoin (NITRO), its co-crystals (A), or the parent mixtures of nitrofurantoin with co-crystallizing agents (B). The permeations were analyzed across monolayers obtained by IEC-6 cells. The permeation of free nitrofurantoin (NITRO) was analyzed across the Millicell filters alone (filters) or coated by monolayers (cells). The cumulative amounts in the basolateral receiving compartments were linear within 60 min ($n=6$, $r \geq 0.990$, $P < 0.001$). The resulting slopes of the linear fits were used for the calculation of permeability coefficients (P_{app}). All data are reported as mean \pm SD of three independent experiments.

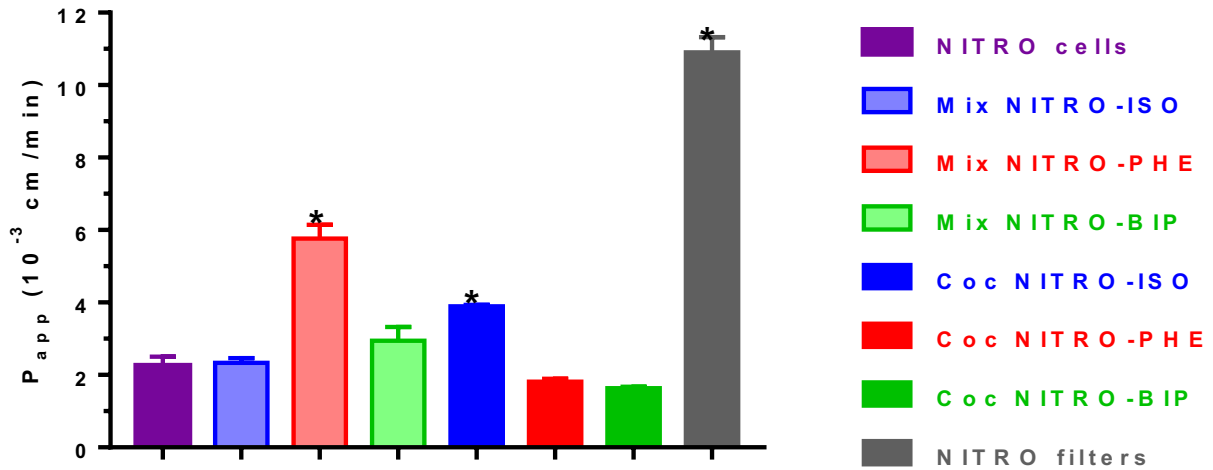


Figure 7. Permeability coefficients (P_{app}) of nitrofurantoin across IEC-6 monolayers after introduction in the “Millicell” apical compartments of powders constituted by free nitrofurantoin (NITRO), its co-crystals, or the parent mixtures of nitrofurantoin with co-crystallizing agents. The permeation of free nitrofurantoin (NITRO) was analyzed across the Millicell filters alone (filters) or coated by monolayers (cells). All data related to permeation studies are reported as the mean \pm SD of three independent experiments. * $P < 0.001$ versus NITRO cells.

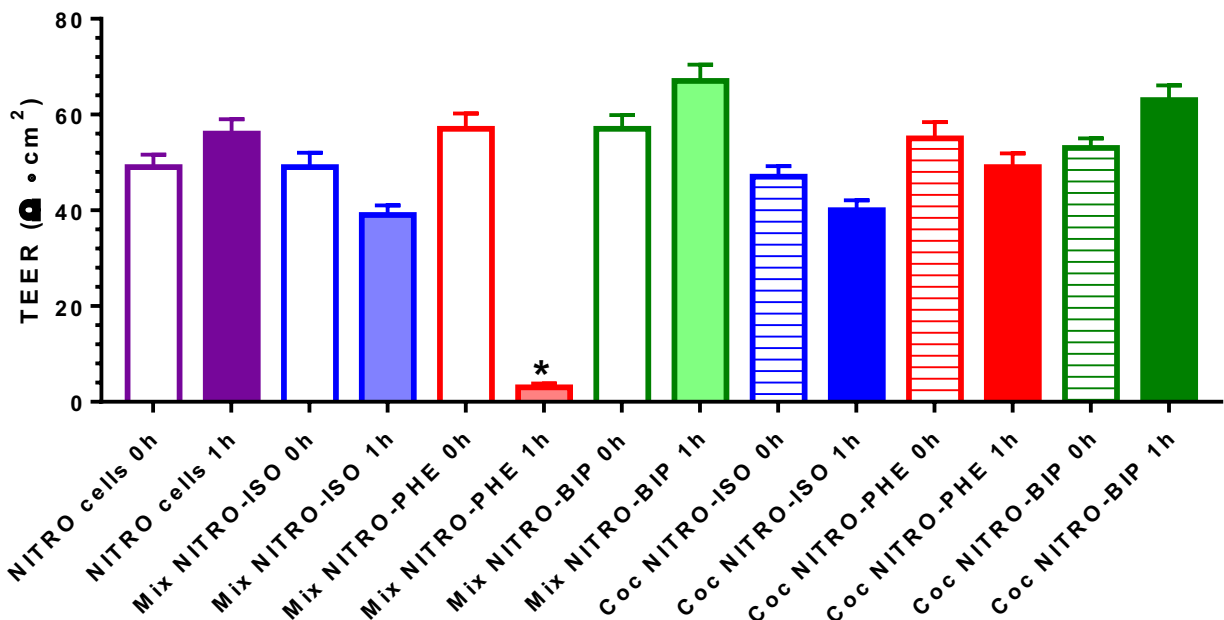


Figure 8. Transepithelial electrical resistance (TEER) values of IEC-6 monolayers obtained when cell cultures reached the confluence. In particular, parallel sets of “Millicell” well plates with similar TEER values were measured before (0 h) and at the end (1 h) of incubation with nitrofurantoin, its co-crystals, and parent physical mixtures. The data are reported as the mean \pm SD of three independent experiments. * $P < 0.001$ versus 0 h.

dissolved from the physical mixtures NITRO-ISO and NITRO-BIP were $2.30 \cdot 10^{-3} \pm 0.13 \cdot 10^{-3}$ cm/min and $2.94 \cdot 10^{-3} \pm 0.38 \cdot 10^{-3}$ cm/min, respectively, appearing therefore not significantly different from the pure nitrofurantoin P_{app} value. Moreover, the TEER values of the IEC-6 monolayers were not significantly changed by the presence of the NITRO-ISO and NITRO-BIP mixtures, as reported in Figure 8. These data indicate that the integrity of IEC-6 monolayers was not altered by the presence of nitrofurantoin both alone and mixed with isoniazid or bipyridyl.

Similar results were obtained with NITRO-PHE and NITRO-BIP co-crystals: indeed, the P_{app} values of nitrofurantoin obtained by their incubation with the monolayers were $1.81 \cdot 10^{-3} \pm 0.08 \cdot 10^{-3}$ cm/min and $1.63 \cdot 10^{-3} \pm 0.04 \cdot 10^{-3}$ cm/min, respectively, resulting not significantly different from the pure nitrofurantoin P_{app} value (Figure 7). Again, the TEER values of the IEC-6 monolayers were not significantly changed by the presence of the NITRO-PHE and NITRO-BIP co-crystals, as reported in Figure 8.

On the other hand, when nitrofurantoin was incubated as NITRO-PHE mixture with IEC-6 monolayers, its P_{app} value was greatly increased, showing a values about three times higher ($5.76 \cdot 10^{-3} \pm 0.39 \cdot 10^{-3}$ cm/min) than that registered for the pure drug ($P < 0.01$). In this case, the P_{app} increase of nitrofurantoin was accompanied by a drastic reduction of the TEER value of the monolayer from $57.0 \pm 3.2 \Omega \cdot \text{cm}^2$, obtained in the absence of the mixture, to $3.1 \pm 0.08 \Omega \cdot \text{cm}^2$, registered after 1 hour of incubation with the mixture ($P < 0.001$). These results clearly indicate that the physical mixture NITRO-PHE was detrimental for the monolayer integrity, inducing a great increase of permeability for nitrofurantoin, even if, interestingly, no alteration of the monolayer was induced by its incubation with the co-crystal NITRO-PHE.

Finally, the incubation of the NITRO-ISO co-crystal with the IEC-6 monolayer induced a significant increase of nitrofurantoin P_{app} value ($P < 0.001$), showing a value about two times higher ($3.89 \cdot 10^{-3} \pm 0.04 \cdot 10^{-3}$ cm/min) than that registered for the pure drug. On the other hand, this

permeability enhancement was not accompanied by a significant alteration of the TEER value of the monolayer, as evidenced in Figure 8. In this case, the ability of NITRO-ISO co-crystal to enhance the permeability of nitrofurantoin across the IEC-6 monolayer does not appear due to a reduction of its integrity.

3.7. Computational Analysis. The two key ingredients modulating the dissolution behaviour of the nitrofurantoin that we can investigate from a computational point of view are: i) the interaction of the drug molecules with the solvent (water) and ii) interaction between drug and co-former molecules in water. By extracting this information from the MD runs of the various systems simulated here (COC, MIX and drug alone, see Computational Details) we can get atomistic insights useful to rationalize the differences in the experimental dissolution profiles of the drug discussed above.

We evaluated the possible changes in the drug-water interaction by calculating the pair radial distribution functions, $g(r)$, between the drug (we selected one carbon atom of NITRO close to the centre of mass) and the centre of mass of all the water molecules for the co-crystals, where the ratio between the drug and co-formers is 4:4 or 4:2 (Section 2.9), and in the physical mixtures, where an excess of co-former is, instead, present; the MD run of the drug alone (NITRO) serves here as a reference. Calculations of the $g(r)$ between selected carbon atoms (chosen to be close to the centre of mass) for both the NITRO and the co-formers in the various systems, provide, on the other hand, information about the tendency of the drug to interact with the considered co-former. The plots are shown in Figure 9.

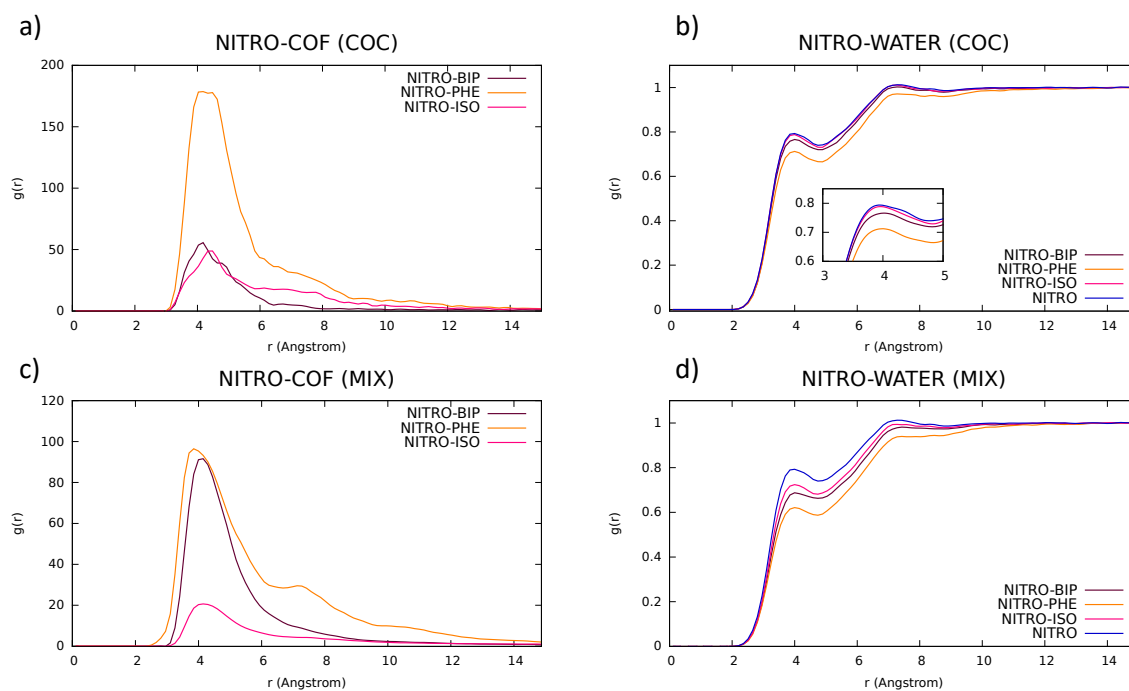


Figure 9. Calculated atom-atom radial distribution functions, $g(r)$, for NITRO-COF and NITRO-WATER in the co-crystals (a and b) and in the physical mixtures (c and d).

By looking at the interaction between nitrofurantoin and the various co-formers in the COC and MIX simulations (panels a and c in Figure 9), it is apparent that, while the interaction of the drug with PHE and ISO seems to be mostly unaffected by the co-former concentration in both strength (related to height of the peaks) and nature (expressed by the position and shape of the curve), in the case of BIP, the interactions become strong only in the mixture, that is passing from 4:2 to 4:20 in the NITRO-COF concentration ratio. For all the systems, the first peak is at around 4-5 Å and, interestingly, the NITRO-PHE MIX curve displays a well-defined second peak at longer distances, suggesting the formation of larger-size aggregates. This second “interaction shell” is absent in the case of BIP and ISO, where only a small shoulder is apparent. Indeed, along the MD trajectories we found stable π -stacked aggregates which involve several PHE units in the NITRO-PHE MIX, the formation of NITRO-BIP dimeric aggregates in the NITRO-BIP MIX and only weak

H-bond (N-H...O) interactions were found for the NITRO-ISO MIX. The initial and final snapshots of the MIX simulations are displayed in Figure 10, where these interactions are highlighted in the insets.

We can complement this analysis by examining the radial distribution functions between the drug and the water molecules (panels b and d in Figure 9) as computed from the COC and MIX MD simulations, respectively. As it could be expected on the basis of the drug-co-former interactions discussed above, the mixture with PHE (Figure 9d) is the one delivering the major effect on the solvation of the drug molecules, with a remarkable reduction in the height of the peak corresponding to the first solvation shell (about 4 Å). Then NITRO-BIP and the NITRO-ISO follow, with the latter giving the less pronounced effect. This trend of the first peak intensity is also found in the COC simulations (Figure 9b), where now the NITRO-ISO curve is almost coincident with the reference $g(r)$ calculated for the drug alone. Interestingly, a more careful look at the data plotted in Figure 9c,d confirms this double-layered interaction of the phenanthroline with the drug, since the NITRO-WATER curve is lower than the reference one also for the second $g(r)$ peak at about 7 Å, while the others show appreciable differences only at short distances. At this point it is important to stress that when comparing the NITRO-WATER $g(r)$ in the MIX simulations with the corresponding function calculated for the 4-cluster molecules extracted from the drug crystal (blue line in Figure 9), the relative heights of the peaks should be considered with caution, in particular in the NITRO-ISO case, where a larger number of molecules (due to the excess of COF) is present, and the diffusion of the drug can be largely affected in a 200 ns MD run.

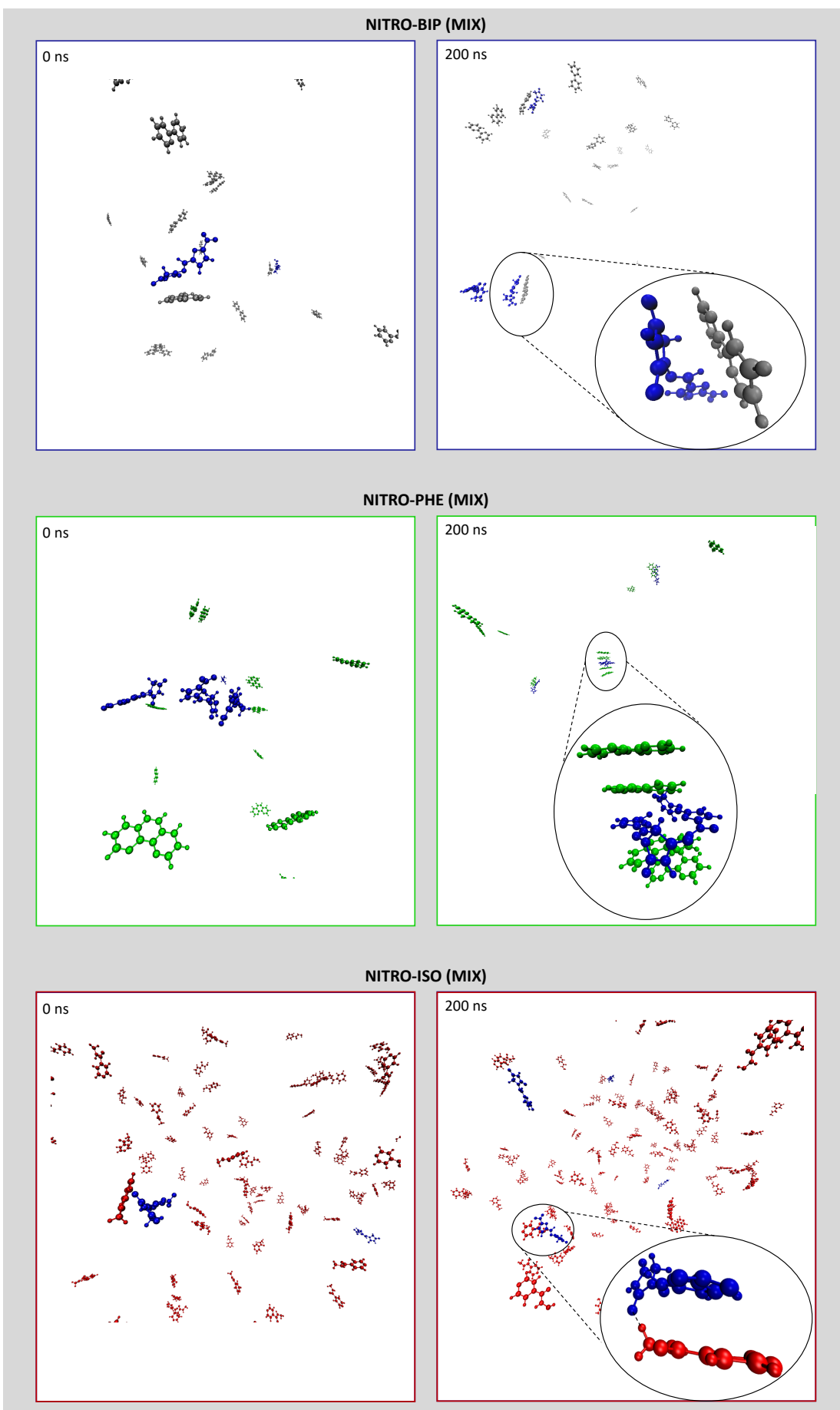


Figure 10. Snapshots extracted at 0 and 200 ns from the MD simulations for the NITRO-BIP, NITRO-PHE and NITRO-ISO mixtures. Water molecules are not shown for clarity. NITRO, BIP, PHE and ISO are in blue, silver, green, and red, respectively.

Data obtained on 400 ns trajectory, reported in Figure S17 in ESI, still show changes in the relative heights of the $g(r)$ peaks, confirming that much longer simulations would be necessary to bring the NITRO-ISO curve closer to the reference $g(r)$ function. In other terms, while the qualitative trend in the predicted change of the drug solvation is reproduced and can be considered as reliable going from the co-crystals to the physical mixtures, quantitative considerations with respect to the solubility of the drug alone can be safely applied only to the COC results.

By combining these findings with the information extracted from the NITRO-COF $g(r)$ (Figure 10 a,c), we can sum up the picture coming from the simulations as follows:

- 1 PHE is the co-former that has the strongest interactions, characterized by π -stacked 4-5 units aggregates, with the nitrofurantoin molecules and it is capable to alter (reduce), in both co-crystal and mixture, the first and second drug solvation shells.
- 2 Similar π -type interaction takes place between the nitrofurantoin and BIP molecules but limited to dimeric structures. These interactions, capable to impact on the first solvation shell of the drug, seem to be concentration-dependent, yielding to a significant reduction of the NITRO solvation only in the case of the physical mixture.
- 3 The highly soluble ISO only weakly interact via H-bonds with the drug and does not seem to alter the dissolution behaviour of the nitrofurantoin.

4. DISCUSSION

FDA guidelines do not consider pharmaceutical co-crystals as New Active Substances (NAS), whereas EMA indicate that they can be considered as NAS with different safety and efficacy properties than APIs, when demonstrated. In this case appropriate registration procedures are required by EMA, an aspect not expected by FDA.^{4,10} The FDA and EMA indications appear controversial if we take into account two important aspects: *i*) in the co-crystal the physicochemical properties of APIs appear modified without altering their molecular structures, thus their therapeutic

and safety properties should be maintained upon solubilization;¹⁰ on the other hand, *ii*) in the crystal lattice, the co-formers are in intimate contact, so it is not easy to define a co-crystal as a physical mixture or a new chemical entity, for which appropriate regulatory procedures are required in order to define its safety and toxicity.^{3,4} Accordingly, we have evidenced that the FT-IR spectra of the pure components of the co-crystals appear unchanged in physical mixtures, differently from co-crystals. The shifts and changes of the peaks evidenced in the IR spectra of co-crystals, and not in the physical mixtures, are related to intimate contacts between their components in the co-crystalline structures at molecular level, able to modify the stretching of their functional groups.

Taking into account that the ability of co-crystals to influence the dissolution pattern of APIs is not the only parameter that can be related to their oral bioavailability, we have also investigated how the co-crystals and their parent physical mixtures would influence the permeation of APIs across the intestinal barrier, simulated *in vitro* by IEC-6 monolayers. The IEC-6 cells derive from primary cells of normal epithelial small intestine of rats,⁶¹ constituting an established, non-transformed cell line able to retain more closely the physiological properties of small intestine than cells derived from tumors. In particular, the IEC-6 cells appear suitable for membrane permeability studies by TEER measurements, allowing to identify the effects of exogenous compounds on the tight-junctions, which are deputed to maintain the membrane integrity.⁶⁰ The dissolution and permeation studies involved the new co-crystal NITRO-ISO and the two previously described co-crystals NITRO-BIP and NITRO-PHE.⁴⁰ About the dissolution studies, we performed six hours of incubation, considering this time of physiologic relevance being compatible with a slow gastrointestinal transit time. For similar reasons, other authors reported dissolution studies of pharmaceutical co-crystals ranging from 60 to 360 minutes.⁶²⁻⁶⁶

About our studies, we have observed that the water solubility of nitrofurantoin was sensibly reduced by phenanthroline in both mixture and co-crystal forms. A similar phenomenon was induced by bipyridyl as mixture, but not as co-crystal, whose impact on nitrofurantoin solubility

appeared weak, similarly to the mixture with isoniazid. The co-crystal of nitrofurantoin with isoniazid allowed to induce a significant increase of the drug solubility in the first 30 minutes of dissolution pattern, which then appeared superimposable with the dissolution pattern of the pure API.

The ideal solubility should be inversely proportional to the melting temperature of the solute;⁶⁷ according to this point of view, the lower melting form of structurally related pharmaceutical compounds should have higher solubility than the other forms. The nitrofurantoin melting point is about 273 °C, higher than those of its co-crystals NITRO-ISO (161 °C) and NITRO-PHE (197 °C) and similar to that of NITRO-BIP (270 °C). On the other hand, the solubility of NITRO-PHE appears lower than that of the free drug, whereas the solubility of NITRO-BIP is higher. Only the co-crystal NITRO-ISO shows an enhanced solubility with respect to nitrofurantoin properly related to a lower melting point (see Table 3 and Figure 5). It is not the first time that poor correlation between melting points and solubility values related to co-crystals was evidenced,^{28,58,68} indicating that the co-crystal solubility is dependent on more than a single factor. Indeed, the correlation between melting temperature and solubility can be generally applied to specific systems, such as the polymorphs, whereas it is considered poorly suitable for co-crystals.⁶⁹

According to the results of the stability studies of solubilized co-crystals, only NITRO-ISO appeared not stable in aqueous environments, suggesting its potential aptitude to easily release nitrofurantoin.

The results obtained by computational analysis contribute to explain the experimental dissolution behaviour of the nitrofurantoin observed in the different systems: the drug solubility is mostly unaffected by the isoniazid, strongly impeded by the phenanthroline and differently impacted by the bipyridyl in the COC (favored) and MIX (disadvantaged) cases. Note that our MD simulations do not provide us with kinetics information about the dissolution process since we “start” our trajectories from already solvated species. We get, on the other hand, atomistic insights on the electrostatic and non-bonded interactions of the various compounds in solution possibly

impacting on the thermodynamics of the dissolution process, when different concentration of drug and co-formers are present. Based on these considerations, we are, therefore, quite confident in interpreting the observed reduction in the drug solubility as arising from a decrease of the thermodynamic activity of the nitrofurantoin, rather than from a decrease in the dissolution rate.

The permeation experiments were performed by using glucose-enriched PBS as the simplest dissolution medium for nitrofurantoin powders. Indeed, differently from simulated intestinal buffers, PBS does not induce TEER changes of the monolayers nor interferes with the activity of efflux transporters expressed on the cell membranes.⁷⁰ At these conditions the IEC-6 monolayers appeared able to behave as a physiologic barrier with TEER values of about $50 \Omega \cdot \text{cm}^2$, as expected for this type of cell lines.⁶⁰ This value was not modified by nitrofurantoin but it was drastically reduced when the drug was mixed with phenanthroline. The mixture NITRO-PHE appeared therefore able to reduce the integrity of the monolayer, and such a reduction was also evidenced by a significant increase of nitrofurantoin permeability when mixed with phenanthroline. The effect of PHE along on the integrity of the IEC-6 cell monolayers could be similar to that reported extensively by Rao and co-workers for Caco-2 cells⁷¹⁻⁷³ where PHE can induce the degradation of the complex occludin-ZO-1 junctional proteins, with a consequent decrease of TEER values of cell monolayers. Conversely, the co-crystal NITRO-PHE did not induce any significant change on both TEER value of the monolayer and permeability of the API. It is not the first time that we have evidenced this type of phenomenon: also mixtures between indomethacin and saccharine²⁸ or carbamazepine and other co-formers²⁹ reduced the monolayer integrity, whereas their parent co-crystals maintained it. On the other hand, we have also previously showed that the co-crystal of indomethacin with 2-hydroxy-4-methylpyridine reduced the integrity of the monolayer, which was also evidenced by a significant increase of the API permeability, whereas any significant change on both TEER value of the monolayer and permeability of the API was induced by the parent physical mixture.²⁸ It seems therefore confirmed that the biological effects of co-crystals and their parent physical mixtures can be drastically different from each other, even if this does not appear as a rule.

Indeed, both the co-crystal NITRO-BIP and its parent physical mixture did not induce any effect of monolayer integrity and API permeability, despite great solubility differences of nitrofurantoin were evidenced when dissolved from the co-crystal or the mixture. A similar behavior was found with the co-crystal and physical mixture of indomethacin with 2-methoxy-5-nitroaniline.²⁸ Interestingly, the stability studies of solubilized mixtures evidenced that NITRO and BIP can easily interact in water as their co-crystalline form, differently from NITRO and PHE that in water did not induce their co-crystal structure. Finally, the co-crystal NITRO-ISO appeared able to increase the permeability of the API across the monolayer without reducing its integrity, whereas the parent physical mixture did not induce any effects on both API permeability and monolayer integrity. A similar result was found for the co-crystal of indomethacin with saccharine²⁸ and with co-crystals of carbamazepine with vanillic acid or succinic acid.²⁹ These effects may be imputable to co-crystals effects on active transport systems of the cells.

It is important to evidence that the co-crystal NITRO-ISO appears able to transiently enhance the nitrofurantoin solubility and to increase its permeability across an intestinal barrier without inducing its damage, showing potential ability to enhance the NITRO bioavailability following oral administration.

5. CONCLUSIONS

In this work, the solubility and permeability properties of the antibacterial drug nitrofurantoin have been evaluated when dissolved from its co-crystals with isoniazid, phenanthroline and bipyridyl co-formers, or from their parent physical mixtures. The dissolution experiments showed that only the co-crystal NITRO-ISO was associated with a significant increase of nitrofurantoin concentration during its first incubation phase; indeed, the presence of phenanthroline, both in co-crystal and in physical mixture, and of bipyridyl in physical mixture, reduces the drug concentration, whereas the API dissolution properties are only slightly improved

by the co-crystallization with bipyridyl or the mixing with isoniazid. MD simulations of model co-crystal and mixtures systems revealed that the detrimental effect of phenanthroline on the API solubility is due to very strong π - π interactions, able to alter both the first and the second solvation shell of the drug in water, regardless the concentration ratio between the drug and the co-former. On the other hand, calculations indicate that bipyridyl can establish significant π -type interactions with nitrofurantoin, reducing its solubility, only when present at high concentration, that is in the case of the physical mixture. No significant effects were evidenced for the isoniazid, which instead shown an initial marked increase in the drug solubility for the co-crystal. It is worthwhile to stress that, due to the small co-crystal clusters adopted in our calculations, we are simulating the “equilibrium” situation, that is the dissolution profile at long timescale, where indeed the NITRO-ISO co-crystal curve does not substantially differ from the one of the nitrofurantoin.

As for the permeation experiments, the physical mixtures NITRO-ISO, NITRO-BIP and the NITRO-PHE, NITRO-BIP co-crystals did not evidence effects neither on the pure nitrofurantoin permeation nor on the TEER values of the IEC-6 monolayers, whereas NITRO-PHE mixture was able to induce a drastic reduction of the TEER value jeopardizing the monolayer integrity. Finally, the incubation of the NITRO-ISO co-crystal showed a significant increase of nitrofurantoin permeation without any significant alteration of the TEER value of the monolayer. These results confirm, as we evidenced in the past,^{28,29} that the co-crystals can induce effects on the permeability and integrity of intestinal monolayers ~~be~~ drastically different than the effects produced by ~~those of~~ their parent physical mixtures or the API alone, suggesting that appropriate regulatory procedures should be required in order to define the safety and toxicity of pharmaceutical co-crystals.

This phenomenon could derive from specific molecular aggregations obtained in water by dissolving the drug from the co-crystal or its physical mixture. In particular, it is suggested that the molecular aggregations obtained by the dissolution of co-crystals can be characterized by conformations different than those obtained by the dissolution of parent physical mixtures or the pure drug. Each type of specific conformation may be able to differently influence the protein

activity of a biological system; as a consequence co-crystals and their parent physical mixtures can produce final specific effects on a physiologic system that be drastically different from each other.

ACKNOWLEDGMENTS

Support from the University of Ferrara, Italy (2019-FAR.L-DA_002) in the frame of the project FAR2019 is gratefully acknowledged. Computational resources were provided by the mésocentre EXPLOR of Université de Lorraine (Project 2018CPMXX0602), the LPCT local computational resource and GENCI-CCRT/CINES (Grant 2020-A0010810139). We would like to thank Mr. Gabriele Bertocchi for assistance with the X-Ray powder diffraction analyses.

REFERENCES

(1) Emami, S; Siahi-Shadbad, M.; Adibkia, K.; Barzegar-Jalali, M. Recent advances in improving oral drug bioavailability by cocrystals. *Bioimpacts* **2018**, 8(4), 305-320. doi: 10.15171/bi.2018.33

(2) Lipinski, C.A.; Lombardo, F.; Dominy, B.W.; Feeney, P.J. Experimental and computational approaches to estimate solubility and permeability in drug discovery and development setting. *Adv. Drug Deliv. Rev.*, **2012**, 64, 4-17. doi: 10.1016/s0169-409x(00)00129-0

(3) Dalpiaz, A; Pavan, B; Ferretti, V. Can pharmaceutical co-crystals provide an opportunity to modify the biological properties of drugs? *Drug Discov. Today* **2017**, 22(8), 1134-1138. doi: 10.1016/j.drudis.2017.01.010

(4) Dalpiaz, A.; Ferretti, V.; Botti, G., Pavan B. Drug release from pharmaceutical co-crystals: are therapeutic and safety properties of active pharmaceutical substances retained? *Curr Drug Deliv.* **2019**, 16(6), 486-489. doi: 10.2174/156720181606190723115802

- (5) Amidon, G.L.; Lennernäs, H.; Shah, V.P.; Crison, J.R. A theoretical basis for a biopharmaceutic drug classification: the correlation of *in vitro* drug product dissolution and *in vivo* bioavailability. *Pharm. Res.* **1995**, 12(3), 413-420. doi: 10.1023/a:1016212804288
- (6) Kalepua, S.; Nekkanti, V. Insoluble drug delivery strategies: review of recent advances and business prospects. *Acta Pharm. Sin. B* **2015**, 5, 442–453. doi: 10.1016/j.apsb.2015.07.003
- (7) Yamamoto, K.; Kojima, T.; Karashima, M.; Ikeda, Y. Physicochemical evaluation and developability assessment of co-amorphouses of low soluble drugs and comparison to the co-crystals. *Chem. Pharm. Bull.* **2016**, 64, 1739-1746. doi: 10.1248/cpb.c16-00604
- (8) Serajuddin, A.T.M. Salt formation to improve drug solubility. *Adv. Drug Deliv.* **2007**, 59, 603-616. doi: 10.1016/j.addr.2007.05.010
- (9) Rodrigues, M.; Baptista, B.; Lopes, J.A.; Sarraguça, M.C. Pharmaceutical cocrystallization techniques. advances and challenges. *Int. J. Pharm.* **2018**, 547, 404-420. doi: 10.1016/j.ijpharm.2018.06.024
- (10) Kumar, A.; Kumar, S.; Nanda, A. A Review about regulatory status and recent patents of pharmaceutical co-crystals. *Adv. Pharm. Bull.* **2018**, 8, 355-363. doi: 10.15171/apb.2018.042
- (11) Kuminek, G.; Cao, F.; Bahia de Oliveira da Rocha, A.; Gonçalves Cardoso, S.; Rodríguez-Hornedo, N. Cocrystals to facilitate delivery of poorly soluble compounds beyond-rule-of-5. *Adv. Drug Deliv. Rev.* **2016**, 101, 143–166. doi: 10.1016/j.addr.2016.04.022
- (12) Duggirala, N.K.; Perry, M.L.; Almarsson, Ö.; Zaworotko, M.J. Pharmaceutical cocrystals: along the path to improved medicines. *Chem. Commun.* **2016**, 52, 640–655. doi: 10.1039/c5cc08216a

(13) Karimi-Jafari, M.; Padrela, L.; Walker, G.M.; Croker, D.M. Creating cocrystals: a review of pharmaceutical cocrystal preparation routes and applications. *Cryst. Growth Des.* **2018**, 18(10), 6370-6387. doi:10.1021/acs.cgd.8b00933

(14) Sanphui, P.; Devi, V.K.; Clara, D.; Malviya, N.; Ganguly, S.; Desiraju, G.R. Cocrystals of hydrochlorothiazide: solubility and diffusion/permeability enhancements through drug–conformer interactions. *Mol. Pharm.* **2015**, 12, 1615-1622. doi: 10.1021/acs.molpharmaceut.5b00020

(15) Saikia, B.; Bora, P.; Khatioda, R.; Sarma, B. Hydrogen bond synthons in the interplay of solubility and membrane permeability/diffusion in variable stoichiometry drug cocrystals. *Cryst. Growth Des.* **2015**, 15, 5593-5603. doi: 10.1021/acs.cgd.5b01293

(16) Dai, X.L.; Li, S.; Chen, J.M.; Lu, T.B. Improving the membrane permeability of 5-fluorouracil via cocrystallization. *Cryst. Growth Des.* **2016**, 16, 4430-4438. doi: 10.1021/acs.cgd.6b00552

(17) Eedara, B.B.; Tucker, I.G.; Zujovic, Z.D.; Rades, T.; Price, J.R.; Das, S.C. Crystalline adduct of moxifloxacin with trans-cinnamic acid to reduce the aqueous solubility and dissolution rate for improved residence time in the lungs. *Eur. J. Pharm. Sci.* **2019**, 136, 104961. doi: 10.1016/j.ejps.2019.104961

(18) Palanisamy, V.; Sanphui, P.; Sainaga Jyothi, V.G.S.; Shastri, N.R.; Bolla, G.; Palanisamy, K.; Prakash, M.; Vangala, V.R. Tuning diffusion permeability of an anti-retroviral drug, emtricitabine, via multicomponent crystallizations. *Cryst. Growth Des.* **2021**, 21, 1548–1561. doi: 10.1021/acs.cgd.0c01344

(19) Banik, M.; Gopi, S.P.; Ganguly, S.; Desiraju, G.R. Cocrystal and salt forms of furosemide: solubility and diffusion variations. *Cryst. Growth Des.* **2016**, 16, 5418-5428. doi: 10.1021/acs.cgd.6b00902

(20) Surov, A.O.; Volkova, T.V.; Churakov, A.V.; Proshin, A.N.; Terekhova, I.V.; Perlovich, G.L. Cocrystal formation, crystal structure, solubility and permeability studies for novel 1, 2, 4-thiadiazole derivative as a potent neuroprotector. *Eur. J. Pharm. Sci.* **2017**, 109, 31-39. doi:10.1016/j.ejps.2017.07.025

(21) Huang, S.; Xue, Q.; Xu, J.; Ruan, S.; Cai T. Simultaneously improving the physicochemical properties, dissolution performance, and bioavailability of apigenin and daidzein by co-crystallization with theophylline. *J. Pharm. Sci.* **2019**, 108, 2982-2993. doi: 10.1016/j.xphs.2019.04.017

(22) Reggane, M.; Wiest, J.; Saedtler, M.; Harlacher, C.; Gutmann, M.; Zotnick, S.H.; Piechon, P.; Dix, I.; Müller-Buschbaum, K.; Holzgrabe, U.; Meinelb, L.; Galli, B..Bioinspired Co-crystals of imatinib providing enhanced kinetic solubility. *Eur. J. Pharm. Biopharm.* **2018**, 128, 290–299. doi: 10.1016/j.ejpb.2018.05.012

(23) Yan, Y.; Chen, J.M.; Lu, T.B. Simultaneously enhancing the solubility and permeability of acyclovir by crystal engineering approach. *Cryst. Eng. Comm.* **2013**, 15, 6457-60. doi:10.1039/c3ce41017j

(24) Machado, T.C.; Gelain, A.B.; Rosa, J.; Cardoso, S.G.; Caon, T. Cocrystallization as a novel approach to enhance the transdermal administration of meloxicam. *Eur. J. Pharm. Sci.* **2018**, 123, 184–190. doi: 10.1016/j.ejps.2018.07.038

(25) do Amaral, L.H.; do Carmo, F.A.; Amaro, M.I.; de Sousa, V.P.; da Silva, L.C.R.P.; de Almeida, G.S.; Rodrigues, C.R.; Healy, A.M.; Cabral, L.M. Development and characterization of dapsone cocrystal prepared by scalable production methods. *AAPS Pharm. Sci. Tech.* **2018**, 19(6), 2687-2699. doi: 10.1208/s12249-018-1101-5

(26) Seo, J.W.; Hwang, K.M.; Lee, S.H.; Kim D.W.; Park E.S. Preparation and characterization of adefovir dipivoxil-stearic acid cocrystal with enhanced physicochemical properties. *Pharm. Dev. Technol.* **2018**, 23, 890-899. doi:10.1080/10837450.2017.1334664

(27) Suzuki, Y.; Muangnoi, C.; Thaweeseest, W.; Teerawonganan, P.; Ratnatilaka Na Bhuket, P.; Titapiwatanakun, V.; Yoshimura-Fujii, M.; Sritularak, B.; Likhitwitayawuid, K.; Rojsitthisak, P.; Fukami, T. Exploring novel cocrystalline forms of oxyresveratrol to enhance aqueous solubility and permeability across a cell monolayer. *Biol. Pharm. Bull.* **2019**, 42, 1004–1012. doi: 10.1248/bpb.b19-00048

(28) Ferretti, V.; Dalpiaz, A.; Bertolasi, V.; Ferraro, L.; Beggiato, S.; Spizzo, F.; Spisni, E.; Pavan B. Indomethacin co-crystals and their parent mixtures: does the intestinal barrier recognize them differently? *Mol. Pharm.* **2015**, 12(5), 1501-1511. doi: 10.1021/mp500826y

(29) Dalpiaz, A.; Ferretti, V.; Bertolasi, V.; Pavan, B.; Monari, A.; Pastore, M. From physical mixtures to co-crystals: how the cofomers can modify solubility and biological activity of carbamazepine. *Mol. Pharm.* **2018**, 15(1), 268-278. doi: 10.1021/acs.molpharmaceut.7b00899

(30) Kumar, A.; Kumar, S.; Nanda, A. A Review about regulatory status and recent patents of pharmaceutical co-crystals. *Adv. Pharm. Bull.* **2018**, 8, 355-363. doi: 10.15171/apb.2018.042

(31) Huttner, A.; Verhaegh, E.M.; Harbarth S., Muller, A.E.; Theuretzbacher, U.; Mouton J.W. Nitrofurantoin revisited: a systematic review and meta-analysis of controlled trials. *J. Antimicrob. Chemother.* **2015**, 70, 2456–2464. doi:10.1093/jac/dkv147

(32) Rosenberg, H.A; Bates, T.R. The influence of food on nitrofurantoin bioavailability. *Clin. Pharmacol. Ther.* **1976**, 20(2), 227-232. doi: 10.1002/cpt1976202227

(33) Novelli, A.; Rosi, E. Pharmacological properties of oral antibiotics for the treatment of uncomplicated urinary tract infections. *J. Chemother.* **2017**, 29, 10-18. doi: 10.1080/1120009X.2017.1380357

- (34) Cherukuvada, S; Babu, N.J.; Nangia, A. Nitrofurantoin–p-aminobenzoic acid cocrystal: hydration stability and dissolution rate studies. *J. Pharm. Sci.* **2011**, 100(8), 3233-3244. doi: 10.1002/jps.22546
- (35) Thakuria, R.; Sarma, B.; Nangia, A. Hydrogen bonding in molecular crystals. In: *Comprehensive Supramolecular Chemistry II*; Atwood, J.L., Ed.; Elsevier, 2017; pp 25-48. doi: 10.1016/B978-0-12-409547-2.12598-3
- (36) Wijma, R.A.; Huttner, A.; Koch, B.C.P.; Mouton, J.W.; Muller A.E. Review of the pharmacokinetic properties of nitrofurantoin and nitroxoline. *J. Antimicrob. Chemother.* **2018**, 73, 2916–2926. doi:10.1093/jac/dky255
- (37) Vangala, R.; Chow, P.S.; Tan, R.B.H. Co-crystals and co-crystal hydrates of the antibiotic nitrofurantoin: structural studies and physicochemical properties. *Cryst. Growth Des.* **2012**, 12, 5925–5938. doi: 10.1021/cg300887p
- (38) Caira M.R.; Pienaar, E.W.; Lotter, A.P. Polymorphism and pseudopolymorphism of the antibacterial nitrofurantoin. *Mol. Cryst. Liq. Cryst.* **1996**, 279, 241–264. doi: 10.1080/10587259608042194
- (39) Zhang, Z.; Cai, Q.; Xue, J.; Qin, J.; Liu, J.; Du, Y. Co-crystal formation of antibiotic nitrofurantoin drug and melamine co-former based on a vibrational spectroscopic study. *Pharmaceutics* **2019**, 11(2), 56. doi: 10.3390/pharmaceutics11020056
- (40) Wang, H.; Xiao, H.; Liu, N; Zhang, B.; Shi, Q. Three new compounds derived from nitrofurantoin: x-ray structures and hirshfeld surface analyses. *Open J. Inorg. Chem.* **2015**, 5, 63-73. doi: 10.4236/ojic.2015.53008
- (41) Otwinowski, Z; Minor, W. Processing of X-ray diffraction data collected in oscillation mode. *Methods in Enzymology* **1997**, 276, 307-326. doi:10.1016/S0076-6879(97)76066-X

- (42) Altomare, A.; Burla, M.C; Camalli, C.; Cascarano, G.; Giacovazzo, C.; Guagliardi, A.; Moliterni, A.G.; Polidori, G.; Spagna, R. SIR97: a new tool for crystal structure determination and refinement. *J. Appl. Crystallogr.* **1999**, 32, 115–119. doi: 10.1107/S0021889898007717
- (43) Sheldrick, G. M. Crystal structure refinement with SHELXL. *Acta Cryst.* **2015**, C71, 3-8. doi: 10.1107/S2053229614024218
- (44) Farrugia, L.J. *WinGX* Suite for small-molecule single-crystal crystallography. *J. Appl. Crystallogr.* **1999**, 32, 837–838. <https://doi.org/10.1107/S0021889899006020>
- (45) Burnett, M.N.; Johnson, C. K. ORTEPIII: Oak Ridge Thermal Ellipsoid Plot Program for Crystal Structure Illustrations. Report ORNL-6895; Oak Ridge National Laboratory: Oak Ridge, TN, USA, **1996**. doi.org/10.2172/369685
- (46) Artursson, P.; Karlsson, J. Correlation between oral drug absorption in humans and apparent drug permeability coefficients in human intestinal epithelial (Caco-2) cells. *Biochem. Biophys. Res. Commun.* **1991**, 175, 880–885. doi: 10.1016/0006-291x(91)91647-u
- (47) Pal, D.; Udata, C.; Mitra, A.K. Transport of cosalane - a highly lipophilic novel anti-hiv agent - across caco-2 cell monolayers. *J. Pharm. Sci.* **2000**, 89, 826–833. doi: 10.1002/(SICI)1520-6017(200006)89:6<826::AID-JPS15>3.0.CO;2-4
- (48) Raje, S.; Cao, J.; Newman, A.H.; Gao, H.; Eddington, N.D. Evaluation of the blood-brain barrier transport, population pharmacokinetics, and brain distribution of benzotropine analogs and cocaine using in vitro and in vivo techniques. *J. Pharmacol. Exp. Ther.* **2003**, 307, 801–808. doi: 10.1124/jpet.103.053504
- (49) Martínez, L.; Andrade, R.; Birgin, E.G.; Martínez, J.M. PACKMOL: a package for building initial configurations for molecular dynamics simulations. *J. Comput. Chem.* **2009**, 30 (13), 2157–2164. doi: 10.1002/jcc.21224

- (50) Götz, A.W.; Williamson, M.J.; Xu, D.; Poole, D.; Le Grand, S.; Walker, R.C. Routine microsecond molecular dynamics simulations with AMBER on GPUs. 1. Generalized born. *J. Chem. Theory Comput.* **2012**, 8(5), 1542–1555. doi: 10.1021/ct200909j
- (51) Salomon-Ferrer, R.; Götz, A.W.; Poole, D.; Le Grand, S.; Walker, R.C. Routine microsecond molecular dynamics simulations with AMBER on GPUs. 2. Explicit solvent particle mesh ewald. *J. Chem. Theory Comput.* **2013**, 9(9), 3878–3888. doi: 10.1021/ct400314y
- (52) Bhogala, B.R.; Basavoju, S.; Nangia, A. Tape and layer structures in cocrystals of some di- and tricarboxylic acids with 4,4'-bipyridines and isonicotinamide. From binary to ternary cocrystals. *CrystEngComm.* **2005**, 7, 551-562. doi: 10.1039/B509162D
- (53) Childs, S.L.; Stahly, G.P.; Park, A. The salt-cocrystal continuum: the influence of crystal structure on ionization state. *Mol. Pharm.* **2007**, 4(3), 323-338. doi: 10.1021/mp0601345
- (54) Domańska, U.; Pobudkowska, A.; Pelczarska, A.; Zukowski, L. Modelling, solubility and pK(a) of five sparingly soluble drugs. *Int. J. Pharm.* **2011**, 403(1-2), 115-122. doi: 10.1016/j.ijpharm.2010.10.034
- (55) Alvarez, S. A cartography of the van der Waals territories. *Dalton Trans.* **2013**, 42(24), 8617-8636. doi: 10.1039/c3dt50599e
- (56) Alhalaweh, A; George, S.; Basavoju, S.; Childs, S.L.; Rizvic, S.A.A.; Velaga, S.P. Pharmaceutical cocrystals of nitrofurantoin: screening, characterization and crystal structure analysis. *CrystEngComm*, **2012**, 14, 5078–5088. doi: 10.1039/c2ce06602e
- (57) Vangala, V.R.; Chow, P.S.; Tan, R.B.H. Co-crystals and co-crystal hydrates of the antibiotic nitrofurantoin: structural studies and physicochemical properties. *Cryst. Growth Des.* **2012**, 12, 5925–5938. doi: 10.1021/cg300887p
- (58) Teoh, X.Y.; Bt Mahyuddin, F.N.; Ahmad, W.; Chan, S.Y. Formulation strategy of

nitrofurantoin: co-crystal or solid dispersion? *Pharm Dev Technol.* **2020**, 25(2), 245-251. doi: 10.1080/10837450.2019.1689401

(59) Pienaar, E.W.; Caira, M.R.; Lötter, A.P. Polymorphs of nitrofurantoin. I. Preparation and X-ray crystal structures of two monohydrated forms of nitrofurantoin. *J. crystallogr. spectrosc. res.* **1993**, 23, 739–744

(60) Gildea, J.J.; Roberts, D.A.; Bush, Z. Protective effects of lignite extract supplement on intestinal barrier function in glyphosate-mediated tight junction injury. *J. Clin. Nutr. Diet.*, 2017, 3,1. doi: 10.4172/2472-1921.100035

(61) Quaroni, A.; Wands, J.; Trelstad, R.L.; Isselbacher, K.J. Epithelioid cell cultures from rat small intestine. Characterization by morphologic and immunologic criteria. *J. Cell. Biol.* 1979, 80, 248-265. doi: 10.1083/jcb.80.2.248

(62) Basavoju, S.; Boström, D.; Velaga, S.P. Indomethacin-saccharin cocrystal: design, synthesis and preliminary pharmaceutical characterization. *Pharm. Res.* **2008**, 25(3), 530-541. doi: 10.1007/s11095-007-9394-1

(63) Jung, M.S.; Kim, J.S.; Kim, M.S.; Alhalaweh, A.; Cho, W.; Hwang, S.J.; Velaga, S.P. Bioavailability of indomethacin-saccharin cocrystals. *J. Pharm. Pharmacol.* **2010**, 62(11), 1560-1568. doi: 10.1111/j.2042-7158.2010.01189.x.

(64) Arafa, M.F.; El-Gizawy, S.A.; Osman, M.A.; El Maghraby, G.M. Xylitol as a potential co-crystal co-former for enhancing dissolution rate of felodipine: preparation and evaluation of sublingual tablets. *Pharmaceutical Development and Technology* **2016**, 23(5), 454–463. doi:10.1080/10837450.2016.1242625

(65) Nugrahani, I.; Auli, W.N. Diclofenac-proline nano-co-crystal development, characterization, in vitro dissolution and diffusion study. *Heliyon* **2020**, 6(9), e04864. doi: 10.1016/j.heliyon.2020.e04864

(66) El-Gizawy, S.A.; Osman, M.A.; Arafa, M.F.; El Maghraby, G.M. Aerosil as a novel co-crystal co-former for improving the dissolution rate of hydrochlorothiazide. *Int J Pharm.* **2015**, 478(2), 773-778. doi: 10.1016/j.ijpharm.2014.12.037

(67) Yalkowsky, S.H. *Solubility and solubilization in aqueous media*; Oxford University Press: New York, Copyright American Chemical Society, 1999.

(68) Good, D.J.; Rodriguez-Hornedo, N. Solubility advantage of pharmaceutical cocrystals. *Cryst. Growth Des.* **2009**, 9(5), 2252–2264. doi: 10.1021/cg801039j

(69) Roy, L.; Lipert, M.P.; Rodriguez-Hornedo, N. Co-crystal solubility and thermodynamic stability. In *Pharmaceutical salts and co-crystals*; Wouters, J., Quere, L., Eds.; Royal Society of Chemistry: Cambridge, 2012; pp 247–279. doi: 10.1039/9781849733502-00247

(70) Ingels, F.; Defermec, S.; Destexhe, E.; Oth, M.; Van den Mooter, G.; Augustijns, P. Simulated intestinal fluid as transport medium in the Caco-2 cell culture model. *Int. J. Pharm.* **2002**, 232, 183–192. doi: 10.1016/s0378-5173(01)00897-3

(71) Rao, R.K.; Basuroy, S.; Rao, V.U.; Karnaky, K.J.Jr; Gupta, A. Tyrosine phosphorylation and dissociation of occludin-ZO-1 and E-cadherin-beta-catenin complexes from the cytoskeleton by oxidative stress. *Biochem J.* **2002**, 368(Pt 2), 471-481. doi: 10.1042/BJ20011804

(72) Rao, R.K.; Li, L.; Baker, R.D.; Baker, S.S.; Gupta, A. Glutathione oxidation and PTPase inhibition by hydrogen peroxide in Caco-2 cell monolayer. *Am J Physiol Gastrointest Liver Physiol.* **2000**, 279(2), G332-340. doi: 10.1152/ajpgi.2000.279.2.G332

(73) Rao, R. Oxidative stress-induced disruption of epithelial and endothelial tight junctions. *Front Biosci.* **2008**, 13, 7210-7226. doi: 10.2741/3223

CAPTION OF FIGURES

Figure 1. Schematic representation of nitrofurantoin and the co-formers isoniazid, 2,2'-bipyridyl and 1,10-phenanthroline in co-crystals NITRO-ISO, NITRO-BIP and NITRO-PHE, respectively.

Figure 2. ORTEPIII³⁶ view for (a) nitrofurantoin/isoniazid (NITRO-ISO); (b) nitrofurantoin/phenanthroline (NITRO-PHE³¹) and (c) nitrofurantoin/2,2'-bipyridyl (NITRO-BIP³¹) co-crystals. Thermal ellipsoids are drawn at the 40% probability level. Hydrogen bonds are drawn as dashed lines.

Figure 3. TGA and DTA traces obtained for pure [A] nitrofurantoin and its co-crystals [B] NITRO-ISO, [C] NITRO-PHE and [D] NITRO-BIP

Figure 4. FT-IR spectra of NITRO-ISO physical mixture [A] and NITRO-ISO co-crystal [B].

Figure 5. Solubility and dissolution profiles in PBS 10 mM at 37 °C for nitrofurantoin as free drug, or co-crystallized, or mixed in the parent mixtures. Data are reported as the mean \pm SD of three independent experiments.

Figure 6. Permeation kinetics of nitrofurantoin after introduction in the “Millicell” apical compartments of powders constituted by free nitrofurantoin (NITRO), its co-crystals (A), or the parent mixtures of nitrofurantoin with co-crystallizing agents (B). The permeations were analyzed across monolayers obtained by IEC-6 cells. The permeation of free nitrofurantoin (NITRO) was analyzed across the Millicell filters alone (filters) or coated by monolayers (cells). The cumulative amounts in the basolateral receiving compartments were linear within 60 min ($n=6$, $r \geq 0.990$, $P <$

0.001). The resulting slopes of the linear fits were used for the calculation of permeability coefficients (P_{app}). All data are reported as mean \pm SD of three independent experiments.

Figure 7. Permeability coefficients (P_{app}) of nitrofurantoin across IEC-6 monolayers after introduction in the “Millicell” apical compartments of powders constituted by free nitrofurantoin (NITRO), its co-crystals, or the parent mixtures of nitrofurantoin with co-crystallizing agents. The permeation of free nitrofurantoin (NITRO) was analyzed across the Millicell filters alone (filters) or coated by monolayers (cells). All data related to permeation studies are reported as the mean \pm SD of three independent experiments. * $P < 0.001$ versus NITRO cells.

Figure 8. Transepithelial electrical resistance (TEER) values of IEC-6 monolayers obtained when cell cultures reached the confluence. In particular, parallel sets of “Millicell” well plates with similar TEER values were measured before (0 h) and at the end (1 h) of incubation with nitrofurantoin, its co-crystals, and parent physical mixtures. The data are reported as the mean \pm SD of three independent experiments. * $P < 0.001$ versus 0 h.

Figure 9. Calculated atom–atom radial distribution functions, $g(r)$, for NITRO-COF and NITRO-WATER in the co-crystals (a and b) and in the physical mixtures (c and d).

Figure 10. Snapshots extracted at 0 and 200 ns from the MD simulations for the NITRO-BIP, NITRO-PHE and NITRO-ISO mixtures. Water molecules are not shown for clarity. NITRO, BIP, PHE and ISO are in blue, silver, green, and red, respectively.